REC-ERC-78-12

STUDIES OF A METHOD TO PREVENT DRAFT TUBE SURGE AND THE ANALYSIS OF WICKET GATE FLOW AND FORCES

Prepared for the Bureau of Reclamation
by the Applied Research Laboratory
Pennsylvania State University, State College, Pennsylvania

Engineering and Research Center
Bureau of Reclamation

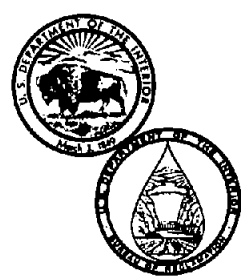

April 1979

MS-230 (1-76)
Bureau of Reclamation

TECHNICAL REPORT STANDARD TITLE PAGE

1. REPORT NO.	2. GOVERNMENT ACCESSION NO.	3. RECIPIENT'S CATALOG NO.
REC-ERC-78-12		

4. TITLE AND SUBTITLE

Studies of a Method to Prevent Draft Tube Surge and the Analysis of Wicket Gate Flow and Forces

5. REPORT DATE
April 1979

6. PERFORMING ORGANIZATION CODE

7. AUTHOR(S)
Walter S. Gearhart, Adam M. Yocum, and Thomas A. Seybert

8. PERFORMING ORGANIZATION REPORT NO.
REC-ERC-78-12

9. PERFORMING ORGANIZATION NAME AND ADDRESS

Applied Research Laboratory
The Pennsylvania State University
P O Box 30
State College, Pennsylvania 16801

10. WORK UNIT NO.

11. CONTRACT OR GRANT NO.
6-07-DR-50160

12. SPONSORING AGENCY NAME AND ADDRESS

Engineering and Research Center
Bureau of Reclamation
Denver, Colorado 80225

13. TYPE OF REPORT AND PERIOD COVERED

14. SPONSORING AGENCY CODE

15. SUPPLEMENTARY NOTES

16. ABSTRACT

An airflow facility was used to simulate the flow through a set of wicket gates and the draft tube typical of a hydroelectric pump-turbine. A method of preventing draft tube surge was studied which consists of injecting some high energy fluid from the spiral casing into the draft tube counter to the direction of the swirl. The results of these tests provide design criteria for selecting injection nozzle configuration and estimating the required injection flow for a turbine of given performance characteristics. A potential solution of the flow through a two-dimensional radial cascade of airfoils also is presented. The predicted flow field characteristics are compared with experimental measurements and the results indicate very good agreement between the measured and predicted values.

17. KEY WORDS AND DOCUMENT ANALYSIS

a. DESCRIPTORS-- / hydraulic machinery/ *hydraulic turbines/ *draft tube surge/ wicket gate forces/ velocity distribution/ hydraulic models/ mathematical models/ flow patterns/ vortices/ potential flow/ surges/ fluid flow

b. IDENTIFIERS--

c. COSATI Field/Group 13B,-13G COWRR: 1313.1

18. DISTRIBUTION STATEMENT	19. SECURITY CLASS (THIS REPORT)	21. NO. OF PAGES
Available from the National Technical Information Service, Operations Division, Springfield, Virginia 22151.	UNCLASSIFIED	73
	20. SECURITY CLASS (THIS PAGE) UNCLASSIFIED	22. PRICE

REC-ERC-78-12

STUDIES OF A METHOD TO PREVENT DRAFT TUBE SURGE AND THE ANALYSIS OF WICKET GATE FLOW AND FORCES

Prepared for the Bureau of Reclamation

by

Walter S. Gearhart

Adam M. Yocum

Thomas A. Seybert

Applied Research Laboratory
Pennsylvania State University
State College, Pennsylvania,
under Contract No. 6-07-DR-50160

April 1979

Hydraulics Branch
Division of Research
Engineering and Research Center
Denver, Colorado

SI METRIC

UNITED STATES DEPARTMENT OF THE INTERIOR * BUREAU OF RECLAMATION

ACKNOWLEDGMENTS

This work was performed at the Applied Research Laboratory of the Pennsylvania State University and sponsored by the Engineering and Research Center, Bureau of Reclamation, Denver, Colorado, as part of the Bureau's Pumped-Storage Research Activities under the Energy Research and Development Program. Special thanks is given to Dr.-Ing H. T. Falvey of the Bureau of Reclamation, Denver, who provided frequent consultation and implemented the exchange of information and hardware required in the completion of this program. The guidance and comments of Dr. G. F. Wislicenus were most helpful in the conceptual and development phases of this effort. The data reported in this document were measured in U.S. customary units and converted to SI metric units.

CONTENTS

TABLES

CONTENTS — Continued

FIGURES

GLOSSARY

A_N	total area of injection nozzles (3 nozzles)
A_T	area of draft tube throat
B	depth of the wicket gate
c	chord length of the wicket gate
D	draft tube inlet diameter
D'	diameter of injection nozzle
f	frequency of the pressure pulsations during surge
F_1, F_2	functions
g	gravitational constant
h	head
k_1	nozzle coefficient
L	draft tube length
L_t	length of injection nozzle throat
N	number of wicket gates
N_R	Reynolds number
P	power
$\sqrt{\overline{p^2}}$	rms value of surge condition
Δp	root-mean-square (rms) pressure pulsation amplitude
Q	flow
Q_B	bypass discharge
Q_T	turbine discharge
r	radial coordinate
r_1	radius to the center of the exit from a wicket gate passage (see fig. 10)
r_i	radius of trailing edge of wicket gates (see fig. 2)
r_s	radius of the wicket gate spindle centers
R	dimensionless radial coordinate, r/c
s	minimum spacing between one wicket gate trailing edge and the adjacent wicket gate (see fig. 10)
S	momentum parameter
S^*	critical momentum parameter
v_r	radial component of velocity
v_{ref}	temporary velocity (variable)
v_x	x component of velocity
v_y	y component of velocity
v_{r_s}	normalizing velocity in the original plane = $Q/2\,\pi B_{r_s}$
v_θ	circumferential component of velocity
$V_{original\ plane}$	dimensionless magnitude of the total velocity vector in the original plane
$V_{transformed\ plane}$	dimensionless magnitude of the total velocity vector in the transformed plane
V_{A_T}	axial velocity in draft tube throat bypass
V_R	dimensionless radial component of velocity v_r/v_{r_s}
V_θ	dimensionless circumferential component of velocity v_θ/v_{r_s}
V_{θ_T}	circumferential velocity in draft tube throat
V_{θ_i}	circumferential velocity at wicket gate exit (see fig. 2)
W_t	width of injection nozzle throat
x, y	dimensionless coordinates of the cartesian coordinate systems
α	flow angle (see fig. 10)
α'	average flow angle leaving the wicket gates
γ	density of water
η	turbine efficiency
θ	angular coordinate in the polar coordinate system expressed in radians
ρ	mass density
ν	kinematic viscosity
ϕ	angle of fluid injection
ϕ_s	speed coefficient

GLOSSARY–Continued

ψ	stream function
ω	angular velocity of the turbine runner
Ω	angular momentum flux

A bar ($\bar{}$) over a variable signifies a mass averaged value.

Subscripts

i	evaluated at the exit of the wicket gates
B	related to bypass flow
T	related to turbine flow
s	spindel of wicket gate
$*$	indicates the critical swirl condition

SUMMARY AND CONCLUSIONS

Injection Nozzle Studies

Experimental studies with respect to eliminating draft tube surge by injecting fluid into the draft tube counter to the existing swirl resulted in the following observations.

- As the ratio of injected fluid Q_B/Q_T is increased, both the surge frequency and the unsteady surge pressure decreases in magnitude.

- The use of various nozzles of a fixed A_N/A_T indicates no measurable change in the effectiveness of the nozzle in reducing or eliminating surge. Similarly, nozzle injection angles up to 45° show no difference in their effectiveness in reducing surge. On this basis, the nozzle geometry would be selected primarily on the basis of hydraulic efficiency and ease of fabrication.

- Empirical data are presented which permits estimating the area of the injection nozzles and the quantity of bleed fluid required for turbines of specified performance characteristics.

- At a given momentum parameter, the quantity Q_B/Q_T required to eliminate surge decreases as higher head turbines or lower specific speed machines are considered.

- Further investigations are required to gather data indicating the influence of draft tube shape on the effectiveness of fluid injection in reducing draft tube surge.

- The hydrodynamic effects, such as cavitation arising from the interaction of the draft tube flow with the high-velocity injection jets, should be experimentally investigated.

Analysis of Flow Field Through Wicket Gates

A two-dimensional potential flow solution has been presented for the flow through a radial cascade, such as the wicket gates of a hydraulic turbine. Comparisons of the predicted flow angles from the potential solution and the angles measured in an air model of a wicket gate system indicate that the potential theory very adequately describes the real fluid characteristics. For the wicket gate system investigated, little difference was found between the potential flow solution and a graphical method currently used. A purely analytical study of cambered wicket gates was conducted which showed a slightly larger deviation between the two methods. It is expected that the potential solution yields the more accurate results, although this conclusion was not verified experimentally. For the present, the main advantages of the potential flow solution are the ability to obtain a more detailed solution of the flow and the ability to include upstream effects if they are considered to be influential. The pressure distribution on the wicket gates is also obtained, and the force and moment coefficients for the wicket gate spindles can be computed.

INTRODUCTION

A study was undertaken to evaluate a proposed method of preventing the occurrence of draft tube surge in hydroelectric pump-turbines. It is generally accepted that the origin of draft tube surge is related to the amount of angular momentum or swirl left in the discharge flow from the turbine. The swirl gives rise to unstable flow patterns, which causes pressure pulsations described as draft tube surge. The adverse consequences of surge are noise, vibration, vertical movement of the runner and shaft, variations in power output, and pressure pulsations in the penstock.

Realizing that the draft tube surge is associated with the amount of swirl present in the discharge flow, the obvious solution would consist of eliminating the swirl. Straightening vanes and fins located in the draft tube have been suggested and tried but have resulted in either efficiency losses or structural and cavitation damage as reported in [1][1]. Injection of air has, in some cases, reduced the magnitude of the pressure pulsations. Appendages attached in the draft tube, such as a hollow cylinder to contain the vortex core or solid fairings to reduce the intensity of the vortex, have met with limited success. The majority of the methods attempted cause excessive energy losses, result in cavitation damage, or induce excessive structural vibrations.

A method is needed that will reduce the rotation in the draft tube flow at off-design conditions without affecting the efficiency of the machine when operating at or near its point of best efficiency. It must not consist of appendages in the draft tube or impair the performance of the machine when it is operating as a pump. The method should be effective with either positive or negative swirl.

The method considered and evaluated in this report consists of a series of flush-mounted nozzles located in the draft tube immediately downstream of

[1] The numbers in brackets refer to listing in the Bibliography.

the turbine rotor. A schematic of the arrangement is shown on figure 1. The nozzles inject fluid in the draft tube counter to the peripheral motion of the discharge flow. Although not shown on figure 1, two separate rows of nozzles could be provided with one row capable of injecting fluid in a direction opposite to that of the other. An arrangement such as this permits the reduction of either positive or negative swirl. It was envisioned that the nozzles would be directly connected to the high-pressure fluid in the spiral casing or penstock. An appropriate system of valving, activated on the basis of wicket gate opening, would control the flow to the nozzles and could control the number of nozzles discharging.

An alternate arrangement to that shown on figure 1 would consist of swirl nozzles individually connected to the spiral casing by separate piping and valving. The flush-mounted nozzles on the wall of the draft tube provide minimum flow disturbance when the swirl nozzles are inactive. The nozzles should not cause a loss in efficiency or cavitation resistance of the machine when they are inactive.

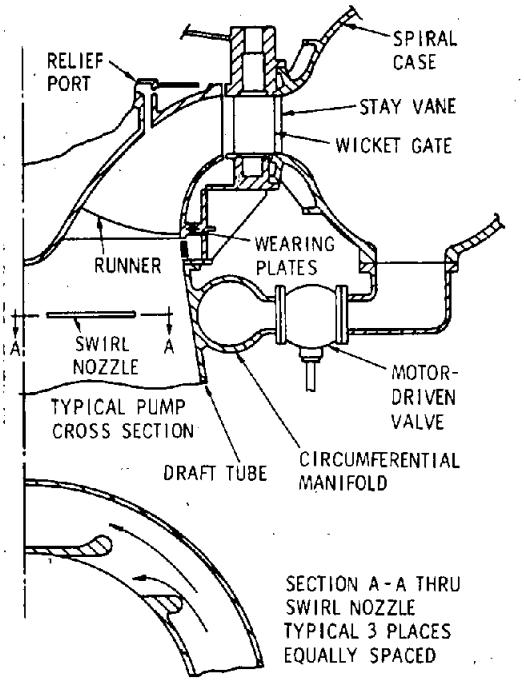

Figure 1. — Schematic of proposed means of preventing draft tube surge.

This report presents an experimental study of the efficiency of various nozzle geometries with respect to the removal of swirl in the draft tube. The resulting empirical data were applied to specific turbine applications to illustrate a method to predict the amount of bypass fluid and to specify the nozzle geometry required to suppress draft tube surge.

Also, a potential solution of the flow through a two-dimensional radial cascade of airfoils is presented, wherein the airfoils in the cascade can be of any arbitrary shape. This solution is applicable to the wicket gates of hydraulic turbines and was developed as an aid in the prediction of draft tube surge. The method of solution consists of transforming the radial cascade into a two-dimensional rectangular cascade by using a conformal transformation. A previously available cascade analysis program, known as the Douglas-Neumann Cascade Program, was utilized to obtain the potential flow solution in the transformed plane. Using a model of a wicket gate and draft tube system, with air as the fluid, experiments to measure the flow angles downstream of the wicket gates were conducted to evaluate the accuracy of the prediction method. A very good correlation was found between the measured and predicted fluid angles. The computer program for solving the flow field through the wicket gates and its application to a typical wicket gate geometry is included as appendix B.

INJECTION NOZZLE STUDIES

Estimate of Bypass Flow

A theoretical estimate of the bypass flow required to implement the proposed means of surge elimination shown on figure 1 shall be established first. This fluid shall be assumed to be piped from the spiral casing and discharged into the draft tube. The bypassing of such fluid represents an energy loss that, for purposes of analysis, will be considered as totally unrecoverable. On this basis, the swirl in the draft tube must be reduced to some specified value with a minimum rate of injected fluid if the described technique is to be successful. An engineering estimate of the ratio of the bypassed flow to the flow through the turbine can be obtained on the basis of momentum considerations.

The momentum parameter S describing the ratio of angular to axial momentum flux in the draft tube is defined in [2]. Figure 2 illustrates the nomenclature and stations considered, where:

$$S = \frac{\Omega D}{\rho Q^2} = \frac{4\, r_i\, V_{\theta i}\, D}{\pi\, \bar{V}_{A_T}\, D^2} \qquad (1)$$

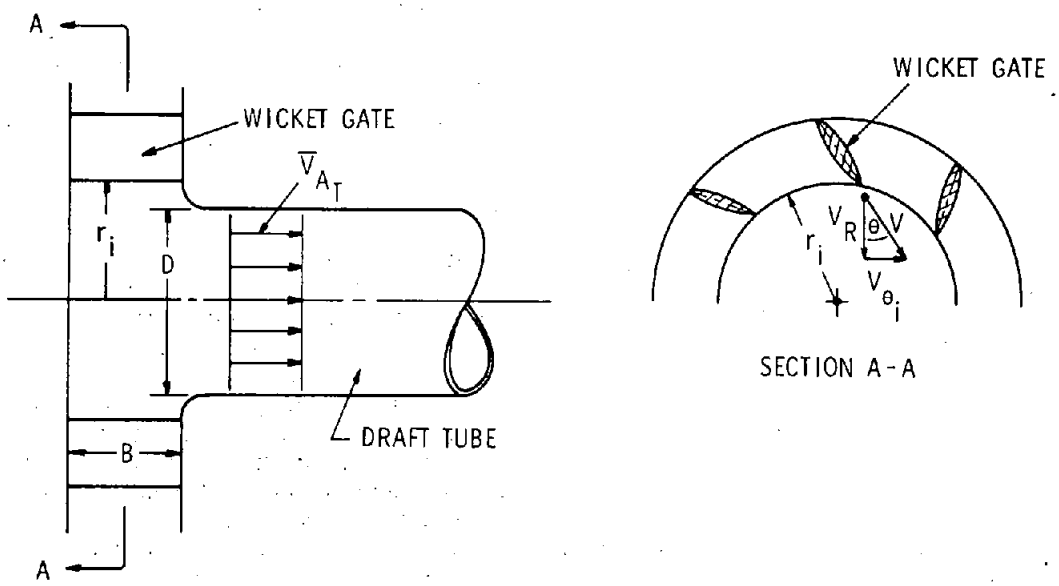

Figure 2. — Schematic of flow leaving wicket gate.

The conservation of angular momentum is assumed constant between the wicket gate exit and the draft tube throat. The quantity $\bar{V}_{A_T}$ represents a mass averaged axial velocity in the draft tube. The assumption is made that the radial distribution of tangential velocity at a given section in the draft tube is represented by a potential vortex. On this basis, the mass averaged quantity $\bar{V}_{\theta_T}$, at a given section of the draft tube would occur at the diameter $\bar{D}$ associated with the mean area of the draft tube. This can be expressed algebraically as:

$$r_i\, V_{\theta_i} = \frac{\bar{D}}{2}\,(\bar{V}_{\theta_T}) = \frac{D}{2(1.414)}\left(\bar{V}_{\theta_T}\right) \qquad (2)$$

and substituted in (1) to give

$$S = \frac{1}{2.22}\left(\bar{V}_{\theta_T}/\bar{V}_{A_T}\right) \qquad (3)$$

It is proposed to reduce the ratio of angular to axial momentum flux that exists in the draft tube at any given gate opening to that level which exists prior to the occurrence of periodic draft tube surge. This level would be attained when the angular momentum of the draft tube flow and that of the injected fluid is summed to give a resultant momentum parameter S, which is less than that at which periodic draft tube surge is predicted to occur, S^*.

If the critical momentum parameter S^* is not to be exceeded in the draft tube, then the amount of fluid that must be directed through the injection nozzles can be evaluated. The quantities of flow and velocity associated with the critical momentum parameter shall be noted by an asterisk. The quantity of bleed fluid required to obtain the critical momentum parameter S^* in the draft tube can be determined by equating the difference between the angular momentum from the turbine discharge $Q_T\, V_{\theta_T}$ and that of the bleed fluid $Q_B\, \sqrt{2gh}$ to the angular momentum at the critical condition $Q_T^* V_{\theta_T}^*$. Thus,

$$\frac{(Q_T\, V_{\theta_T})}{(Q_T^*\, V_{A_T}^*)} - \frac{Q_B\, \sqrt{2gh}}{(Q_T^*\, V_{A_T}^*)} = \left[\frac{Q_T^*\, V_{\theta_T}^*}{Q_T^*\, V_{A_T}^*}\right] = 2.22\, S^* \qquad (4)$$

Equation (4) can be rearranged to provide a ratio of bypass flow to draft tube flow in terms of the momentum parameters S and S^* as

$$\frac{Q_B}{Q_T} = \frac{2.22\ V^*_{A_T}\left[S\left(\frac{V_{A_T}}{V^*_{A_T}}\right) - S^*\left(\frac{V^*_{A_T}}{V_{A_T}}\right)\right]}{\sqrt{2gh}} \qquad (5)$$

The decrease in efficiency $\Delta\eta$ of the turbine due to bleeding bypass fluid to the injection nozzles, assuming that none of the bypass fluid energy is recovered, is:

$$\Delta\eta = 100\left(\frac{Q_B}{Q_T}\right) \qquad (6)$$

If eq. (5) is considered for a given S, the numerator is essentially constant, independent of turbine head. This is based on the assumption, for cavitation purposes, that the velocity at the design condition in the draft tube throat for conventional turbine installations has some upper limit. The ratio of Q_B/Q_T specified by (5) decreases as some reciprocal function as head is increased. On this basis, eq. (6) indicates the decrease in efficiency, due to bleeding bypass fluid to the swirl nozzles, will be less in a high head turbine than in a low head turbine. The performance characteristics for a turbine, such as presented for the Grand Coulee Third Powerplant units [3], provides the quantities required for eq. (5) to estimate the ratio of bypass to draft tube flow at a given momentum parameter.

Test Apparatus

Investigations on the performance of various injection nozzle geometries were conducted in an airflow facility which is shown on figure 3. Similar studies [2, 4] have shown that the use of air as a working fluid has been quite successful in characterizing the momentum parameter in draft tube flow and in predicting the occurrence of draft tube surge. The main air supply was provided by a variable-speed, centrifugal blower and was measured by an orifice meter arrangement. The metered airflow was diffused as it entered the stilling chamber; screens were used to reduce flow turbulence across the stilling chamber flow field. The air entered the cylindrical draft tube radially through wicket-gate-type swirl vanes. The angle between the vanes and a radial line could be set at any angle between 0°

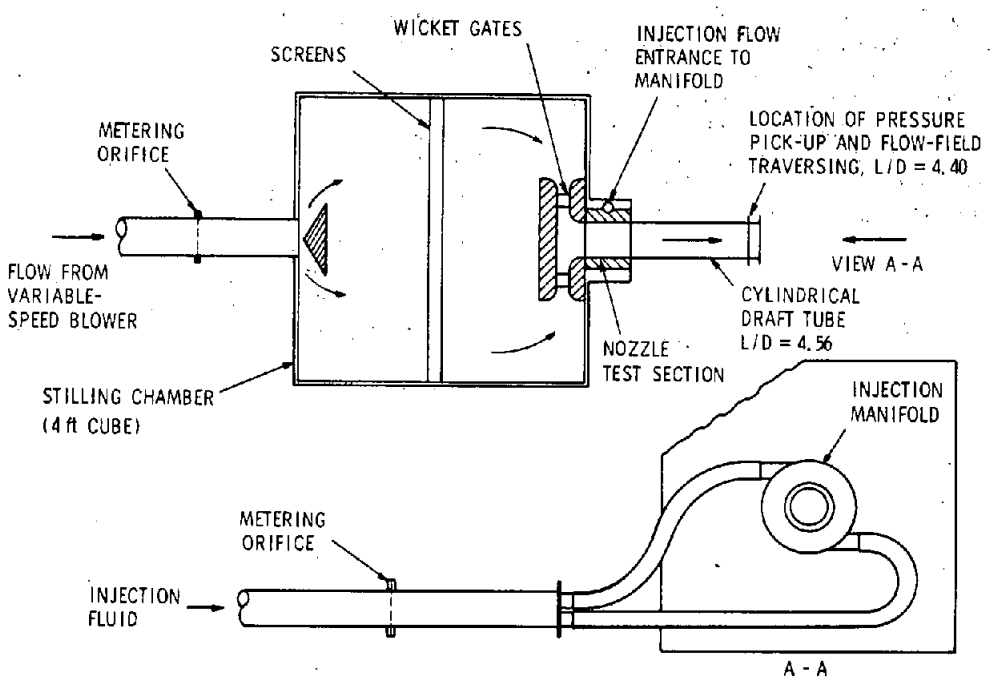

Figure 3. — Schematic of airflow facility.

(radial position) and 82.5° (closed position). It can be shown that the dimensionless momentum parameter $\Omega D/\rho Q^2$ reduces to $K(\tan \alpha')$ for this test facility, where K = constant and α' is the average flow angle leaving the wicket gates. Traverse data across the trailing edge of the wicket gates, using a prism probe, were used to determine flow angles for various wicket gate settings. These data were used to develop a relationship for the momentum parameter as a function of gate setting. Injection fluid provided by an auxiliary air supply and measured by an orifice meter arrangement entered the manifold of the injection nozzle test section located just below the wicket gates. Any ratio of injection fluid flow Q_B, to fluid flow through the gates (turbine flow) Q_T could be provided by the proper setting of a butterfly valve on the auxiliary air supply blower. The nozzle test section provided three points of fluid injection equally spaced in a circumferential plane perpendicular to the draft tube centerline. Nozzle geometries tested are shown in table 1. It should be pointed out that in table 1, A_N, nozzle area, was defined as the sum of the three separate nozzle areas. After passing through the nozzle test section, the airflow entered the cylindrical draft tube (L/D = 4.56). Pressure taps and probe holes were located all along the length of the tube. The cylindrical draft tube could be replaced with an elbow-type (i.e., Fontenelle) draft tube.

The unsteady pressure produced by the swirling flow in the draft tube was monitored at the last pressure tap (L/D = 4.40) on the draft tube by a dynamically calibrated differential pressure transducer. The pressure signal was sent to a Spectral-Dynamics real-time analyzer in conjunction with an ensemble averager from which the frequency f of the surging condition could be established.

Table I

NOZZLE SHAPES TESTED

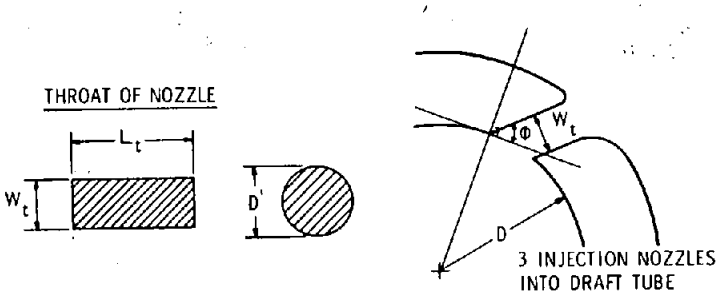

Table 1. — *Nozzle shapes tested*

Nozzle number	Injection angle, ϕ (deg)	Nozzle area, A_N (mm²)	Nozzle area, A_N (in²)	A_N/A_T (%)	L_t/W_t
1	30	38.1	1.500	5.09	8.0
2	↓	19.0	0.750	2.54	4.0
3	↓	9.5	0.375	1.27	0.5
4	↓	28.6	1.125	3.84	1.5
5	0	19.0	0.750	2.54	1.0
	15	↓	↓	↓	↓
	30	↓	↓	↓	↓
	45	↓	↓	↓	↓
6	30	4.8	0.188	0.64	4.0
7	↓	19.0	0.750	2.54	0.25
8	↓	15.5	0.610	2.04	circle*
9	↓	33.7	1.325	4.48	circle**
10	↓	9.5	0.375	1.27	1.0
11	↓	↓	↓	↓	4.0
12	↓	↓	↓	↓	0.25
13	↓	38.1	1.50	5.04	1.0
14	↓	↓	↓	↓	4.0
15	↓	↓	↓	↓	0.25

* D' = 12.7mm (0.5 in)
** D' = 19.0mm (0.75 in)

Figure 4 shows typical data received from the analyzer. The rms (root mean square) value, $\sqrt{\overline{p^2}}$, of the surging condition was read from an rms meter after the signal was passed through a line filter with a characteristic 48 dB per octave rolloff. The band pass of the filter was set at 20 to 120 Hz for all tests. The frequency of all observed pressure surges was between 35 and 70 Hz. Directly across from the draft tube pressure pickup tap was a probe hole used for flow field measurements. A prism probe was used to obtain total pressure, static pressure, and fluid flow angle as a function of radial distance across the draft tube for various flow conditions. The basic parameters used in this study to describe the surging condition were the dimensionless groups suggested by Falvey and Cassidy [5], namely pressure parameter $D^4\sqrt{\overline{p^2}}/\rho Q^2$ and frequency parameter fD^3/Q.

Discussion of Experimental Results

The effect of various fluid injection angles and nozzle geometries was investigated on the basis of their effectiveness in reducing the unsteady pressure amplitude measured in the draft tube. All tests were at Reynolds numbers above 80,000 as recommended in reference [4] and at velocities low enough to prevent compressible effects. A typical spectral analysis indicating the reduction in the amplitude of the unsteady surge pressure is shown on figure 4. It is apparent that both the amplitude and the frequency of the surge are reduced as the ratio of Q_B/Q_T is increased. The spectral analysis indicates no pressure peaks at a Q_B/Q_T of 16 percent indicating that surge has been eliminated at this condition of fluid injection.

The angle of fluid injection ϕ as defined in table 1 was studied with respect to its effect on reducing surge for a given swirl in the draft tube. The four angles of injection investigated were: 0°, 15°, 30°, and 45° (see table 1). The nozzle geometry used in these tests was No. 5, described in table 1, and the results are shown on figure 5 for an S (momentum parameter) of 0.8 and 1.18. The most significant result is that, up to the 45° angle tested, the reduction of surge pressure amplitude is independent of injection angle. The lower end points of the curves on figure 5 represent that ratio of Q_B/Q_T required to completely eliminate surge and it is evident that the quantity of Q_B/Q_T required is equal for the four injection angles tested.

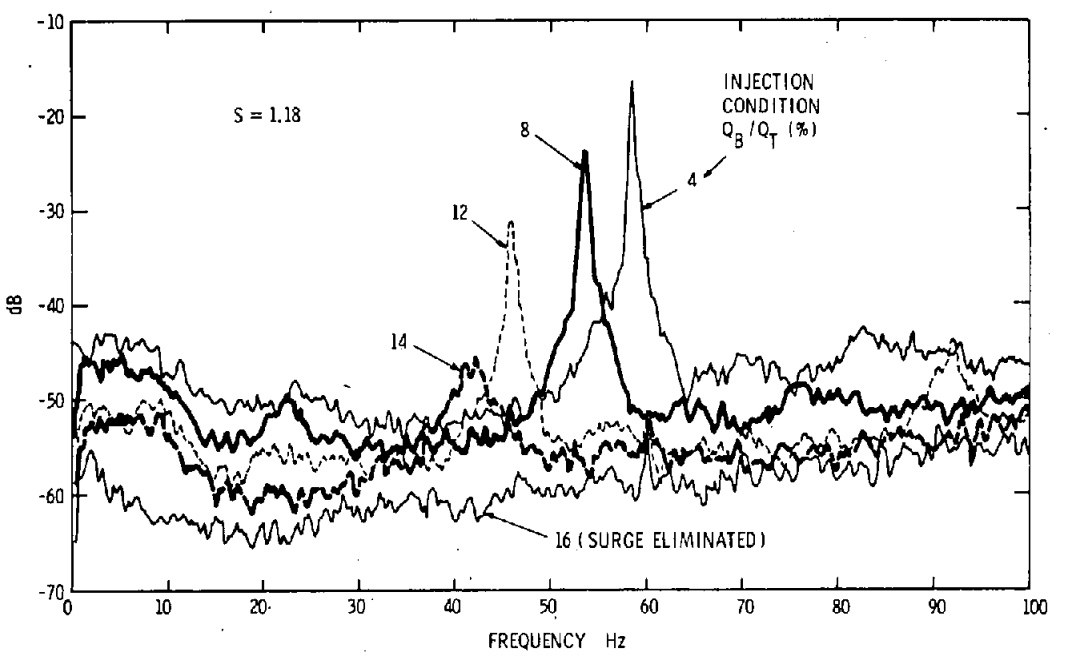

Figure 4. — Spectral analysis of surge.

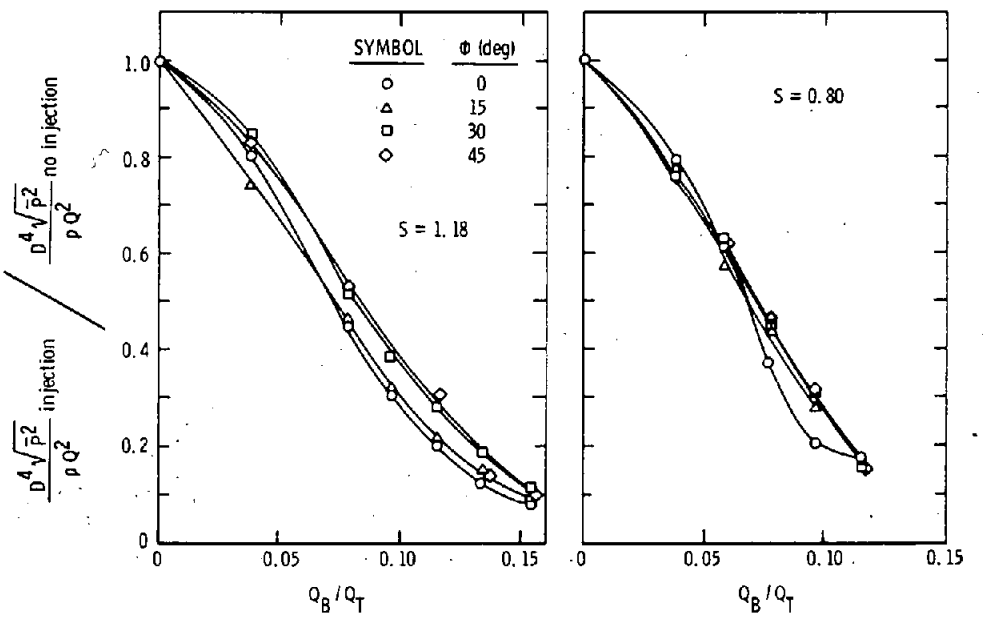

Figure 5. — Comparison of nozzle angle of injection.

An injection angle ϕ of 30° was selected for the tests to investigate the effects of the length-to-width ratio of the injection nozzle as well as the ratio of the area of the injection nozzles to the draft tube throat area. The ratio Q_B/Q_T is plotted against the surge pressure parameter for a series of nozzle geometries at the momentum parameters on figure 6. The lower extremity of each curve represents a condition where surge is eliminated and thereby indicates the ratio of Q_B/Q_T required to eliminate surge for a given A_N/A_T ratio. Figure 6 illustrates that for a given ratio of Q_B/Q_T, the reduction in the surge pressure amplitude is greater as A_N/A_T decreases. This results directly from the fact that to inject a given ratio of Q_B/Q_T into the draft tube, the head and, hence, the velocity must increase as A_N/A_T decreases. Since the momentum of the injected fluid increases as the square of the spouting velocity from the nozzles, smaller ratios of Q_B/Q_T are required to eliminate surge as the head on the turbine increases.

Table 1 lists the nozzle geometries tested and defines their characteristic dimensions. The rather surprising result was that for the L_t/W_t nozzles tested, no measurable difference was observed in the ratio of Q_B/Q_T required to eliminate surge at a given A_N/A_T. This result suggests that the choice of a nozzle geometry to obtain a given A_N/A_T would consist of selecting that geometry which would give the least hydraulic losses and permit the easiest fabrication. On this basis, a cylindrical nozzle which would be elliptical at its intersection with the barrel of the draft tube would seem appropriate.

The tangential and axial velocity components of the flow in the draft tube were measured at a station of L/D = 4.40 indicated on figure 3 by means of a prism probe, which provided a time averaged reading of the local static, total pressure, and flow angularity. The velocity distributions are shown on figure 7 for momentum parameter values of 0.24, 0.41, 0.80, and 1.18. The dashed line in these figures represents similar traverse data having the wicket gates at a setting corresponding to a momentum parameter of 0.8, but with fluid injected to eliminate surge. It is evident that the reversal of axial flow at the axis of rotation is eliminated and considerable swirl has been removed from the flow when fluid is injected.

Without injection, the outer portion of the flow approaches a free vortex or constant angular momentum distribution with solid body rotation near the center. The peripheral velocity distribution downstream of a turbine runner may deviate from that indicated on figure 7. The effect of such variation has not been investigated in the present studies but deserves future consideration.

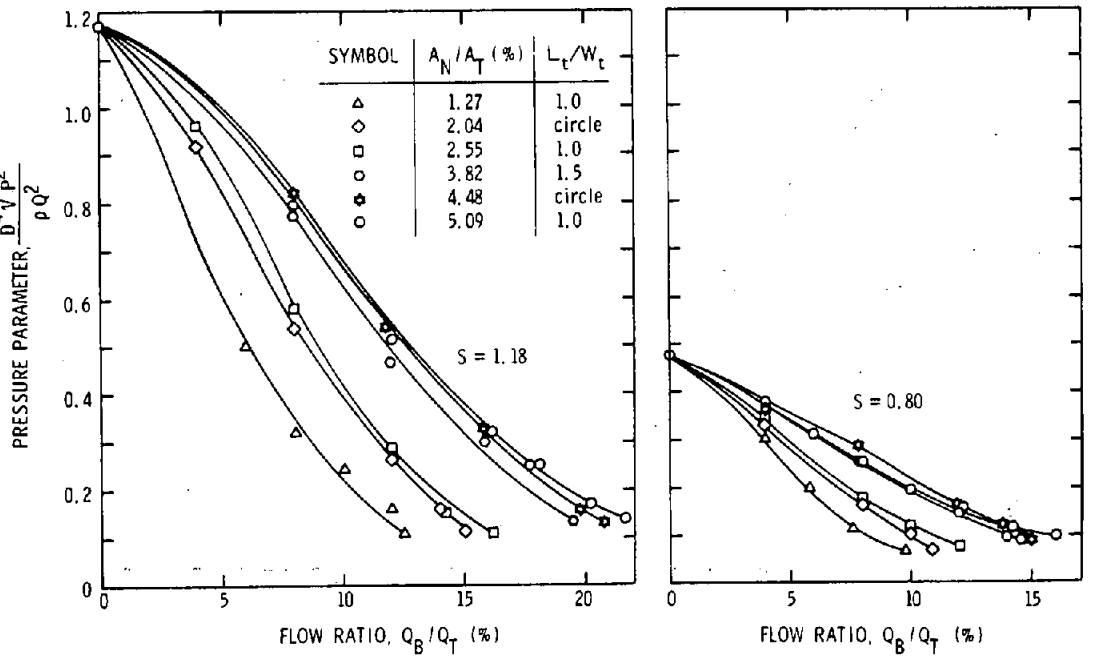

Figure 6. — Comparison of nozzle geometries.

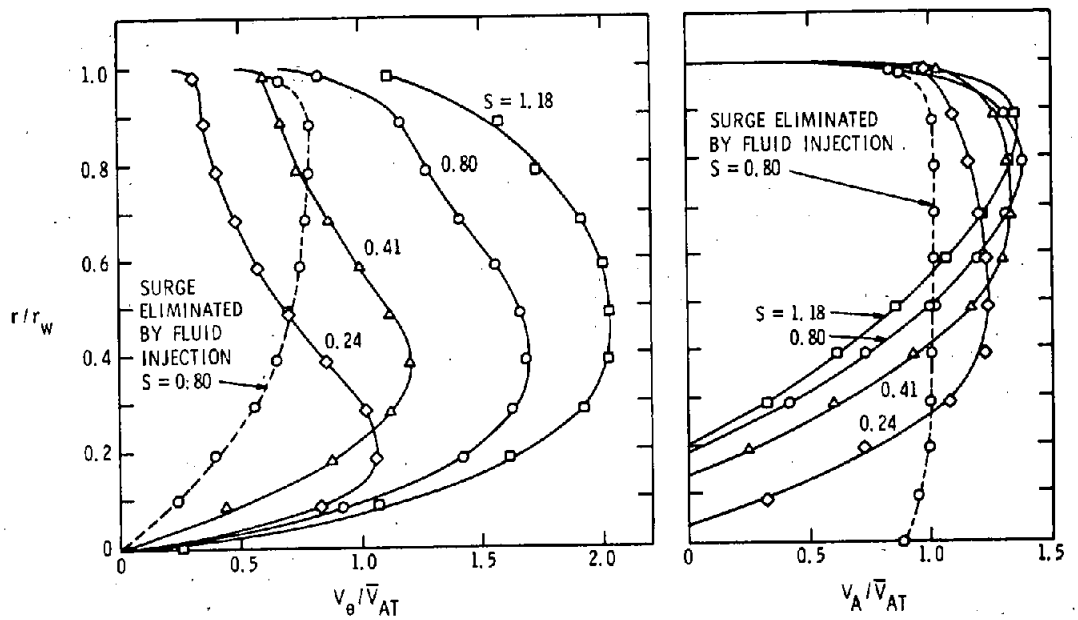

Figure 7. — Axial and tangential velocity distribution.

Comparison of Test Results with Predictions

The ratio of bleed flow to turbine flow was previously derived in eq. (5), assuming ideal momentum transfer between the injected and draft tube flow. On the basis of the preceding experimental data, it is possible to obtain an empirical relation that applies to pump-turbines. The bypass flow can be expressed as:

$$Q_B = K_1 (2gh)^{1/2} A_N \qquad (7)$$

Where K_1 is a nozzle coefficient and assumed equal to 0.9.

The flow through the turbine can be written as:

$$Q_T = \frac{1}{\eta}\left(\frac{P}{h\gamma}\right) \qquad (8)$$

The ratio of bleed flow to turbine flow is then

$$\frac{Q_B}{Q_T} = 39\,100\ \eta \frac{A_T}{P}\left(\frac{A_N}{A_T}\right) h^{3/2}\ \underline{\text{SI}}$$

$$\frac{Q_B}{Q_T} = 451\ \eta \frac{A_T}{P}\left(\frac{A_N}{A_T}\right) h^{3/2}\ \underline{\text{INCH-POUND}} \qquad (9)$$

Experimental data results indicate that for a given A_N/A_T, the ratio of Q_B/Q_T required to eliminate surge at the two S values are shown on figure 8. A curve fitting of this data indicates the following relationship:

For $S = 1.18$

$$\frac{Q_B}{Q_T} = 0.719\left(\frac{A_N}{A_T}\right)^{0.401} \qquad (10)$$

For $S = 0.80$

$$\frac{Q_B}{Q_T} = 0.473\left(\frac{A_N}{A_T}\right)^{0.366} \qquad (11)$$

Using a value of $S = 1.18$, it is possible by substituting (10) in (9) to obtain a relation for Q_B/Q_T of,

$$\frac{Q_B}{Q_T} = \frac{1}{2054\left(\frac{\eta A_T}{P}\right)^{0.67} h}\ \underline{\text{SI}} \qquad (12)$$

$$\frac{Q_B}{Q_T} = \frac{1}{104.7\left(\frac{\eta A_T}{P}\right)^{0.67} h}\ \underline{\text{INCH-POUND}}$$

In similar fashion, the substitution of (11) in (9) provides a relation of Q_B/Q_T for $S = 0.8$

$$\frac{Q_B}{Q_T} = \frac{1}{1460\left(\frac{\eta A_T}{P}\right)^{0.578} h^{0.867}}\ \underline{\text{SI}} \qquad (13)$$

$$\frac{Q_B}{Q_T} = \frac{1}{111.5\left(\frac{\eta A_T}{P}\right)^{0.578} h^{0.867}}\ \underline{\text{INCH-POUND}}$$

An elbow-type draft tube was also evaluated to indicate the influence of draft tube shape. The draft tube tested was similar to the Fontenelle configuration described in [4]. The data and equations relating A_N/A_T to Q_B/Q_T required to eliminate surge for this draft tube are shown on figure 9. By applying the same analysis as indicated for the cylindrical draft tube, the ratio of bypass flow to turbine flow for the elbow-type draft tube was calculated. Using performance, geometrical data, and a speed coefficient ϕ_s of 0.8 for the model of the Grand Coulee Third Powerplant units given in [3], the bypass flow rates were determined for a cylindrical and an elbow-type draft tube. The results are shown in table 2.

Table 2. — *Grand Coulee Third Powerplant bypass flow rates*

	$S = 0.8$	$S = 1.18$
Predicted Ideal-Eq. 5	$Q_B/Q_T = 6.35\%$	$Q_B/Q_T = 5.62\%$
Empirical (cylindrical)	$Q_B/Q_T = 10.3\%$	$Q_B/Q_T = 13.9\%$
Empirical (elbow)	$Q_B/Q_T = 11.5\%$	$Q_B/Q_T = 13.0\%$

The above comparison indicates that the empirically derived quantity of Q_B/Q_T required to eliminate surge at $S = 1.18$ is about 2.5 times

greater than that predicted assuming an ideal momentum transfer. At S = 0.80, the difference between the empirical and estimated values of Q_B/Q_T is not as great. The availability of performance characteristics and geometries of other existing or new turbine installations would permit making similar estimates of the required Q_B/Q_T to eliminate surge at the specified values of momentum parameter.

It should be emphasized that solution of eq. (12) and (13) in conjunction with figure 8 also specifies the A_N/A_T required, for a given turbine, to eliminate surge at a value of S equal to 0.8 or 1.18.

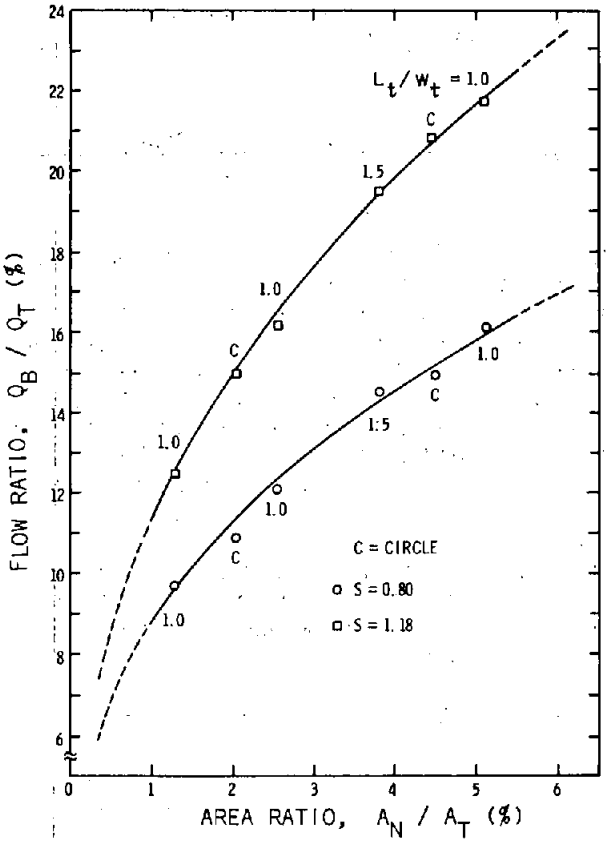

Figure 8. — Injected flow required to eliminate surge for cylindrical draft tube.

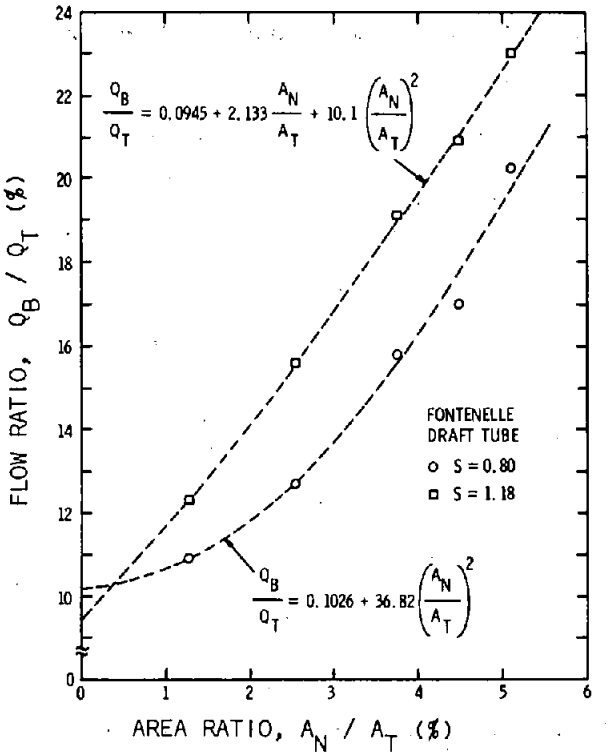

Figure 9. — Injected flow required to eliminate surge for elbow draft tube.

ANALYSIS OF FLOW FIELD THROUGH WICKET GATES

Preliminary Assumptions and Governing Equations

Experimental studies have shown that for a given draft tube shape, the frequency and pressure parameters are independent of N_R (Reynolds number) for Reynolds numbers greater than 1 X 10^5 [2, 5, 6]. This is an important consideration, since turbine prototype Reynolds numbers exceed 1 X 10^5, and, thus, studies of surge can be conducted eliminating N_R as a variable. It has also been found experimentally [2, 5, 6] that, for a particular draft tube, the frequency and pressure parameters correlate with the momentum parameter; and a critical value of the momentum parameter $\Omega D/\rho Q^2$ exists above which surge will occur. These facts have enabled extensive studies to be conducted on

models of various types of draft tubes and for different values of L/D, from which the pressure and frequency parameters can be correlated with the momentum parameter and used to predict surge for prototype installations [4].

The most convenient way to evaluate the momentum parameter is to determine the angular momentum of the flow leaving the wicket gates and subtract from this value the angular momentum removed by the turbine runner. The momentum parameter for the flow in the draft tube can thus be written as:

$$\frac{\Omega D}{\rho Q^2} = \left[\frac{\Omega D}{\rho Q^2}\right]_i - \frac{PD}{\rho \omega Q^2} \qquad (14)$$

where:

P = power output of turbine

ω = angular velocity of the turbine runner

The first term on the right is the momentum parameter for the flow leaving the wicket gates and is currently evaluated using the graphical approach [5] and is illustrated by figure 10. Using this approach, the flow is assumed to leave the wicket gates perpendicular to the minimum cross section between the trailing edge of one wicket gate and the adjacent wicket gate. Referring to the nomenclature defined in figure 10, the momentum parameter at the exit of the wicket gates can be computed by the following expression:

$$\left[\frac{\Omega D}{\rho Q^2}\right]_i = \frac{D\, r_1 \sin \alpha}{BNs} \qquad (15)$$

where:

B = depth of the wicket gates.

N = number of wicket gates.

s, r_i, α } defined on figure 10.

The second term on the right of eq. (14) represents the change in angular momentum across the turbine runner and is evaluated from the turbine performance characteristics usually obtained from model studies.

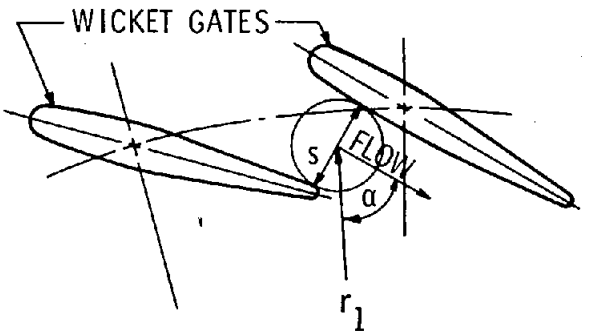

Figure 10. — Schematic of two wicket gates illustrating the graphical method of determining the flow angle and, hence, the momentum parameter.

Although the most convenient way of calculating the momentum parameter is to use the approach expressed by eq. (14), references in [3] and [4] indicate that the graphical method of evaluating the first term of eq. (14) may seriously affect the accuracy of using the momentum parameter to correlate experimental data and to predict the occurrence and characteristics of draft tube surge. For this reason, it was felt that more attention must be given to the details of the flow through the wicket gates. It was also realized that the upstream stay vanes or the inlet spiral may influence the flow leaving the wicket gates; however, these factors obviously cannot be accounted for until an analysis was employed which considered the details of the actual flow process, which is beyond the capability of the graphical approach.

With the above considerations in mind, the following presents a method to obtain a potential solution of the flow through the wicket gates and presents the results of an experimental study conducted to evaluate the accuracy of this approach. A potential flow solution was developed because it represents the first step usually taken in a problem of this nature, which can be used as a basis for a more exact model, if necessary. Since the flow through the

wicket gates is an accelerating flow, the potential flow solution is expected to yield quite satisfactory results by itself.

Several methods for analyzing the potential flow through two-dimensional rectangular cascades are presently available. One of the most general of these, capable of handling airfoils of any arbitrary shape, is a method developed at Douglas Aircraft Corporation and referred to as the Douglas-Neumann Cascade Program. A conformal transformation of a radial flow cascade to a rectangular cascade enables the use of the Douglas-Neumann Cascade Program to analyze the flow in the transformed plane.

The first assumption required to analyze the flow through the wicket gates is that the flow is two-dimensional. For most turbine installations this is a very reasonable assumption, since the wicket gates themselves are two-dimensional, and the flow at the wicket gate inlet and exit is predominately two-dimensional. A schematic of a turbine cross section is presented in figure 11, showing the spiral case, stay vanes, wicket gates, turbine runner, and draft tube. This figure illustrates that the flow passage in the region of the wicket gates is usually a straight section, which is the justification for assuming the flow is two-dimensional. Using the two-dimensional flow assumption, the geometry of a segment of the wicket gate system to be analyzed is presented (fig. 12). Figure 12 also indicates the coordinate system used.

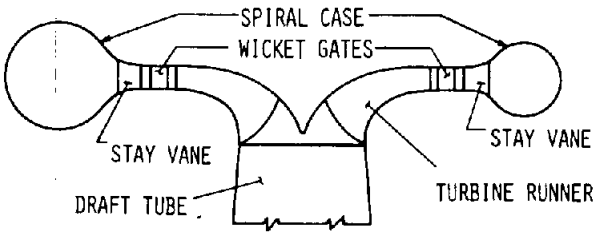

Figure 11. — Schematic of a turbine cross section illustrating the geometry of the flow passage in the region of the wicket gates.

The other necessary assumptions are those which are required to enable the flow to be considered a potential flow. It is therefore assumed that there are no body forces and that the flow is steady, incompressible, inviscid, and irrotational. The inviscid flow assumption is the only assumption requiring some justification. Because the flow is accelerating through the wicket gates, the effects of the boundary layers will be minimal, and thus, an inviscid solution is actually quite realistic in this situation.

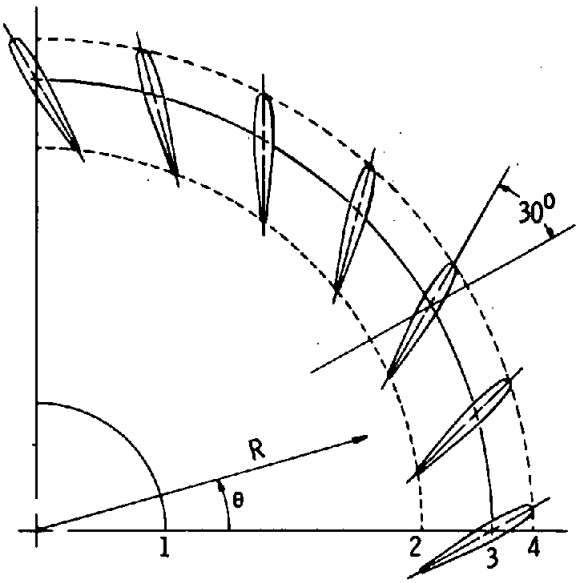

Figure 12. — Schematic of a sector of a wicket gate system in the real coordinate system.

With the above assumptions, the governing equations for the flow are the equation for zero vorticity and the continuity equation. These equations expressed in polar coordinates and in terms of dimensionless variables are as follows:

$$\text{Zero vorticity:}\quad \frac{\partial V_\theta}{\partial R} + \frac{V_\theta}{R} - \frac{1}{R}\frac{\partial V_R}{\partial \theta} = 0 \qquad (16)$$

$$\text{Continuity:}\quad \frac{\partial V_R}{\partial R} + \frac{V_R}{R} + \frac{1}{R}\frac{\partial V_\theta}{\partial \theta} = 0 \qquad (17)$$

A stream function ψ is defined, such that by its definition it satisfies the continuity equation.

$$V_R = \frac{1}{R}\frac{\partial \psi}{\partial \theta} \qquad (18)$$

$$V_\theta = -\frac{\partial \psi}{\partial R} \qquad (19)$$

Substituting eq. (18) and (19) into eq. (16) yields the familiar Laplace equation in polar coordinates.

$$\frac{\partial^2 \psi}{\partial R^2} + \frac{1}{R}\frac{\partial \psi}{\partial R} + \frac{1}{R^2}\frac{\partial^2 \psi}{\partial \theta^2} = 0 \qquad (20)$$

Equation (20) is solved indirectly through a transformation to obtain the flow field solution through the wicket gates. The boundary conditions which must be satisfied in conjunction with eq. (20) are:

1. A specified flow direction at infinity or far upstream.
2. The wicket gates must constitute a streamline, or in other words, the velocity normal to the wicket gate surface must be zero.
3. The Kutta condition must be satisfied at the trailing edge of the wicket gates.

Transformation of the Flow Field

A conformal transformation was used to transform the wicket gate system into a two-dimensional linear cascade, so that the flow in the transformed plane could be analyzed using available procedures. Since the flow in the original plane is considered a potential flow and the transformation in conformal, the flow in the transformed plane is also a potential flow and can be analyzed accordingly. The transformation used is as follows:

$$y = \theta \qquad (21)$$

$$x = \ln R \qquad (22)$$

By applying the chain rule and eq. (21) and (22), it is found that eq. (20) is transformed into Laplace's equation in cartesian coordinates, eq. (23).

$$\frac{\partial^2 \psi}{\partial x^2} + \frac{\partial^2 \psi}{\partial y^2} = 0 \qquad (23)$$

where:

Velocity component in the x direction,

$$v_x = \frac{\partial \psi}{\partial y} \qquad (24)$$

Velocity component in the y direction,

$$v_y = -\frac{\partial \psi}{\partial x} \qquad (25)$$

The transformation of eq. (20) into eq. (23) was carried out to illustrate that, with the transformation employed, the flow in the transformed plane is indeed a potential flow and, thus, obeys the same fundamental laws as the flow in the original plane. In the actual flow analysis, the wicket gates were transformed, and the linear cascade of airfoils obtained were analyzed as if this plane were the real plane. The transformation is illustrated by figure 13, where the wicket gate geometry previously shown in figure 12 is shown in the transformed plane. The circular arcs labeled 1, 2, 3, and 4 in figure 12 become veritcal lines of constant x value in figure 13 and are similarly labeled for a comparison of the two planes. It is interesting to note that the arc of $R = 1$ becomes the y-axis of the cartesian coordinate system in the transformed plane, while the point at $R = 0$ corresponds to $x = -\infty$ in the new plane.

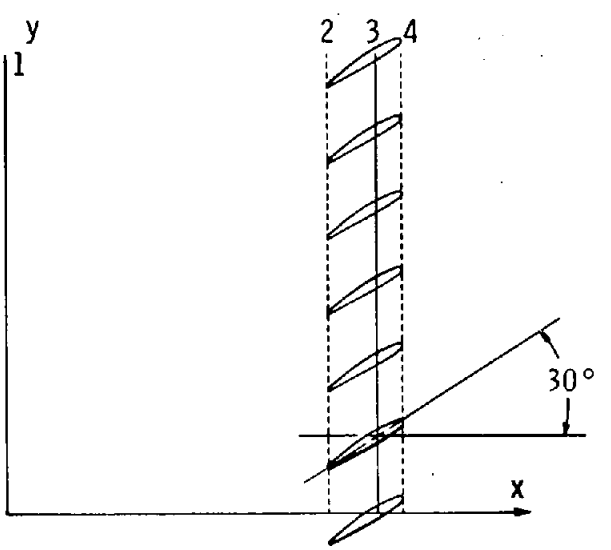

Figure 13. — Schematic of the two-dimensional cascade obtained by transforming the wicket gate system.

Similarly, radial lines of the original plane become lines of constant y value in the transformed plane. The x-axis corresponds to the radial line at $\theta = 0$.

The boundary conditions in the transformed plane are identical to those in the real plane. Since flow angles are not changed by a conformal transformation, the specified inlet flow angles are the same in both planes. In addition, the velocity component normal to the surface of the transformed airfoil must be zero, and the Kutta condition must be satisfied, as in the original plane.

Relationships between the velocity components in the two planes can be found by applying the chain rule and eq. (21) and (22) to the derivatives of ψ with respect to θ and R. It is first found that:

$$\frac{\partial \psi}{\partial \theta} = \frac{\partial \psi}{\partial y} \tag{26}$$

and,

$$\frac{\partial \psi}{\partial R} = \frac{1}{R} \frac{\partial \psi}{\partial x} \tag{27}$$

From eq. (26) and (27) and the definitions of the stream function, the desired relations between the velocities in the two planes are obtained:

$$V_R = \frac{1}{R} V_x \tag{28}$$

$$V_\theta = \frac{1}{R} V_y \tag{29}$$

The relationship between the magnitudes of the total velocity vectors can then be expressed as:

$$V_{original\ plane} = \sqrt{V_R^2 + V_\theta^2} \tag{30}$$

$$= \frac{1}{R} \sqrt{V_x^2 + V_y^2} = \left(\frac{1}{R}\right) V_{transformed\ plane}$$

Method of Solution in the Transformed Plane

The Douglas-Neumann cascade solution [7] was used for analyzing the flow through the transformed cascade because this method of solution is capable of handling infinite cascades of airfoils of an arbitrary shape. A solution is obtained by applying a distribution of sources on the surface of the airfoils in the cascade, such that the combination of the onset velocity, the source at the particular point, and the induced velocity from the remaining source distribution satisfy the boundary condition of zero normal velocity at the surface. In a similar manner, the vorticity distribution on the airfoils is obtained by employing the same set of equations with the velocity vector of the sources rotated 90°.

The source distribution is determined by representing the airfoils as a series of straight-line segments, with the source strength assumed constant over each segment and the boundary condition satisfied at the segment midpoint. With this approximation, the induced velocity at the midpoint of a particular segment can be represented by a summation of a set of integrals representing the induced velocity from the remaining segments. Since the source strength is assumed constant over the segment, the integrals can be evaluated analytically, which results in a set of algebraic equations that must be solved simultaneously for the source strength of each segment. This technique will approach an exact solution as the number of segments approaches infinity, but sufficient accuracy is achieved as long as the straight-line segments are small enough to adequately describe the airfoil shape.

The solution to the general problem is obtained by calculating the potential flow for three basic flows consisting of the solution for a flow with zero angle of attack, 90° angle of attack, and a pure circulatory flow. These three solutions, which all satisfy the boundary condition of a zero velocity component normal to the surface, are then combined in such a manner to satisfy the specified inlet angle and the Kutta condition. The complete solution enables the velocity components and the static pressure to be determined at any point in the flow field, and also yields the overall angle by which the cascade turns the flow.

Discussion of Normalizing Parameters and the Reverse Transformation

Thus far, the equations governing the flow in both planes have been presented, and the method of obtaining a solution in the transformed plane has

been discussed. The equations relating the velocity components in the two planes have also been given. However, before these equations can be specifically applied, consistent normalizing velocities must be selected in each plane. Since it is known from the conservation of mass equation that the average x component of velocity is constant both upstream and downstream of a rectangular cascade, $\bar{v}_x$ represents a convenient parameter to normalize the velocity in the transformed plane. Although the Douglas-Neumann cascade solution uses as a normalizing parameter the modulus of the average velocity vector upstream and downstream of the cascade, the output can easily be converted so that the velocity is normalized by $\bar{v}_x$.

In the original plane, the velocity component corresponding to $\bar{v}_x$ is the radial component. The average radial velocity component is not constant, but, once again from the conservation of mass equation, it is known that $r\,\bar{v}_r$ = constant. Using this relationship, if a reference value of r is selected, a corresponding reference value of $\bar{v}_r$ can be obtained. The value of r which is convenient for this purpose is the radius of the wicket gate spindle centers, r_s. Selecting r_s as the reference radius results in the following definition of the normalizing velocity in the original plane.

$$v_{r_s} = \frac{Q}{2\pi B r_s} \tag{31}$$

It is apparent from the definition that v_{r_s} represents the average radial velocity which would exist at the spindle radius if the wicket gates were not present.

Rewriting eq. (28) in terms of dimensional quantities allows the relationship between the velocities in the planes to be determined when they are normalized using the above parameters. For the present, v_x will be normalized by the temporary variable, v_{ref}

$$\frac{v_r}{v_{r_s}} = \left(\frac{c}{r}\right)\frac{v_x}{v_{ref}} \tag{32}$$

To relate the two normalizing velocities, it is known that v_x should equal $\bar{v}_x$ when $v_r = v_{r_s}$ and $r = r_s$. Solving eq. (32) for v_{ref} after inserting these values yields

$$v_{ref} = \bar{v}_x\left(\frac{c}{r_s}\right) \tag{33}$$

Substituting eq. (33) back into eq. (32) provides the new relationship for relating the dimensionless radial velocity in the original plane to the x component of velocity in the transformed plane.

$$V_r = \frac{v_r}{v_{r_s}} = \left(\frac{c}{r}\right)\frac{v_x}{\bar{v}_x\,\frac{c}{r_s}} = \left(\frac{r_s}{r}\right)\frac{v_x}{\bar{v}_x}$$

$$= \left(\frac{R_s}{R}\right)\frac{v_x}{\bar{v}_x} \tag{34}$$

Similarly,

$$V_\theta = \frac{v_\theta}{v_{r_s}} = \left(\frac{R_s}{R}\right)\frac{v_y}{\bar{v}_x} \tag{35}$$

and,

$$V = \frac{v_{original\ plane}}{v_{r_s}}$$

$$= \left(\frac{R_s}{R}\right)\frac{v_{transformed\ plane}}{\bar{v}_x} \tag{36}$$

These equations provide the necessary relationships for the reverse transformation of the solution from the transformed plane to the original plane. It should be noted that the fluid angles are not changed by the transformation; thus, the above equations need only to be applied when interested in the velocity magnitudes. Eq. (36) is used in the computer program to transform the local velocity on the surface of the blades, thus enabling the pressure distribution on the wicket gate to be determined. The definition of the pressure coefficient employed and sample results are presented in appendix B with the description of the computer program.

Analytical Study Conducted

The method of transforming the wicket gates and employing the rectangular cascade analysis to obtain a potential flow solution was used to analyze the flow through the wicket gates of an air model. This model, which was primarily fabricated to conduct draft tube surge studies, is described in the section on the experimental study. The wicket gates shown in figure 12 are a scale drawing of the real wicket gates in the model. These wicket gates have no

camber, a chord length of 39.7 mm (1.562 in), and a maximum thickness of 5.44 mm (0.214 in).

Solutions were obtained for the wicket gates with angular settings between 0 and 80° in 10° increments. These angles are measured between the wicket gate chord and a radial line. The closed position is at the angular setting of 83°. Two solutions were obtained for each wicket gate setting, one with the flow entering radially and the other solution with the flow at a zero angle of attack in the transformed plane. These two solutions were obtained to evaluate the influence of the upstream flow on the fluid exit angle. It was found that for the present wicket gate geometry, the inlet angle did not affect the exit angle. This conclusion cannot be made for all systems, however, since even for a potential flow solution the spacing between gates will affect the amount of turning the cascade can perform. The present method of solution could be used by testing various spacings to determine what spacing is needed to eliminate upstream effects.

The graphical method indicated by figure 10 was also carried out, and these results are presented along with the experimental results and potential flow solution. Initial results comparing the fluid exit angles predicted by the graphical approach and the potential flow solution revealed very little difference. The question was then raised, would cambered wicket gates demonstrate a larger deviation between the fluid angles predicted using the two methods? To study this possibility, an analytical study was conducted for cambered wicket gates similar to the study for the symmetrical wicket gates. For this case, the results from the potential solution also revealed no significant dependence on the inlet angle. However, a slightly larger deviation was found between the fluid exit angle predicted by the potential solution and the graphical approach. The actual numerical results is presented in the section on analytical and experimental results.

Experimental Program

A sketch of the test facility used to obtain experimental data for comparison with the potential flow solution is shown on figure 14. In this facility, flow surveys were made at a constant radius behind several wicket gate channels, with measurements made every 1.5°. In addition to the open inlet configuration shown in the figure, tests were also conducted with an inlet spiral installed. The tests with and without the inlet spiral enabled the effects of the inlet flow angle on the exit flow from the wicket gates to be investigated. The draft tube has an inlet diameter of 156 mm (6.125 in) and the probe was located at a diameter of 229 mm (9.0 in).

Total pressure, static pressure, and the flow angles were measured using a three-hole prism-type probe. The flow angle was determined by nulling the probe. The total pressure was measured from the center hole, and the static pressure was calculated from the average pressure of the two side holes and a pressure coefficient obtained during a static pressure calibration of the probe. All pressures were measured with a variable-reluctance differential pressure transducer with the voltage output measured by an integrating digital voltmeter.

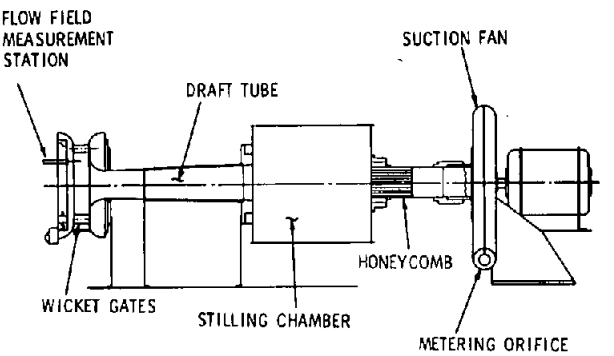

Figure 14. — Sketch of the wicket gate and draft tube model used to experimentally evaluate the potential flow solution.

The velocity magnitude and flow angles, which varied across a wicket gate channel, were used to calculate the momentum parameter by numerically integrating the flow characteristics across a channel to obtain the flow rate and the angular momentum flux. This momentum parameter was then used to calculate an average flow angle for comparison with the theoretical predictions. For a flow with uniform velocity, it can be shown that the only flow characteristic influencing the momentum parameter is the flow angle, as expressed by the following relation:

$$\frac{\Omega D}{\rho Q^2} = \frac{D}{2\pi B}\left(\tan \alpha'\right) \qquad (37)$$

where:

α' = the flow angle for a uniform flow, or the average flow angle for a non-uniform flow yielding the equivalent moment parameter.

All other symbols have been previously defined.

Eq. (37) was used for calculating α' from the momentum parameter obtained experimentally. An average flow angle was also calculated by simply computing the arithmetic average of all the measured local flow angles. These two average angles were almost identical, however, and future references to the average angle will not mention the method of calculation.

Discussion of Analytical and Experimental Results

The downstream flow angle obtained from the potential flow solution in the transformed plane is the angle of the uniform flow theoretically achieved at negative infinity. For all practical purposes, however, uniform flow of constant angularity is achieved a short distance from the trailing edge of the blades. When applying the potential flow solution to a real situation, the flow may or may not become uniform before it reaches the location of the turbine runner. It should be pointed out that even if sufficient spacing for the flow to become uniform is not available, the uniform flow angle still applies for calculating the momentum parameter, since no change in the momentum parameter will occur between the trailing edge and the location where uniform flow would be achieved. With this in mind, the flow angle calculated by the potential theory for the symmetrical wicket gate is presented on figure 15 as a function of wicket gate angle. The angles from the potential theory are represented by the solid line.

The average fluid angles obtained experimentally are also presented on figure 15. No difference was found in the measured angles for the two sets of tests conducted both with and without the inlet spiral; thus, only one set of data is presented. The fact that the exit flow angles did not change with the different inlet configurations is consistent with the predicted data which also showed no effect with the change in the angle of attack.

The graphical method for predicting the momentum parameter, indicated by figure 10, was used to calculate the exit flow angle from the wicket gates to provide an additional comparison and demonstrate whether any improvement is achieved by the potential flow solution. The flow angle α defined on figure 10 is not the average flow angle, however, since the angle is defined within the wicket gate passage and does not represent the angle obtained when the flow becomes uniform. The angle α can be used with eq. (15) to calculate the momentum parameter, and then with the momentum parameter the

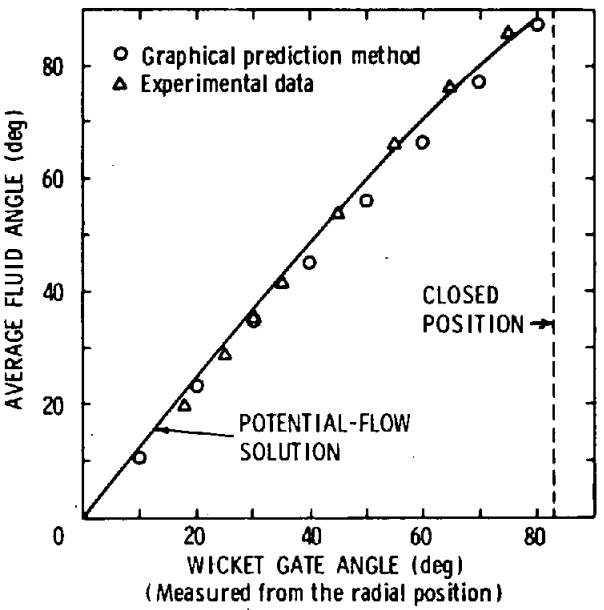

Figure 15. — Average flow angle versus wicket gate angle obtained from the potential flow solution, graphical prediction method, and experimental data.

average flow angle α' can be calculated from eq. (37). The average flow angles calculated in this manner are the data represented by the circles on figure 15.

For the system with the symmetrical wicket gates, as shown by figure 15, the results from both the potential flow solution and graphical method agree very closely with the experimental data. At the higher wicket gate angles the potential solution is only approximately 1° low in its prediction of the fluid angle. At the lower wicket gate settings the potential solution predicts values approximately 2° higher than the measured angles. On the other hand, the graphical method shows its greatest deviation at the higher wicket gate angles, where flow angle is under-predicted by approximately 4°. At the lower wicket gate angles, the fluid angles from the graphical method and the experimental data are approximately equal.

With the deviation between the predicted and experimental data of such a small magnitude, it is difficult to conclude whether the deviation is due to a minor shortcoming of the prediction methods or due to an error in the experimental data. The fact that the experimental data does not appear to be exactly approaching the origin leads one to believe the deviation may be due to experimental error. At

the lower wicket gate angles the probe traverses were nearer to the trailing edge of the wicket gates, and some measurements were, therefore, made with the probe partially in the wakes of the gates. If the measurements were not perfectly centered around the wakes, the error in the angle measurements would not be completely canceled out by the averaging process, resulting in one possible source of error. An additional source of error could be the angle of the wicket gates. The linkage, which controls the angles of the wicket gates, has some hysteresis, which may be enough to allow the gates to be at a slightly different angle than expected.

Over the full range of wicket gate angles the potential solution appears to be slightly more accurate than the graphical method for the symmetrical wicket gate geometry. However, the very small difference between the predictions by both methods and the experimental data does not give one method a significant advantage over the other. It was for this reason that an analytical study of a system with cambered wicket gates was undertaken to determine whether the two methods differ more significantly for cambered wicket gates. The geometry of the wicket gate selected for the study is shown in appendix B, since this wicket gate geometry is also used to document the computer program. The results from the study are presented on figure 16, where the fluid angles predicted by the two methods are plotted similarly to the previous data. Figure 16 shows a slightly larger difference between the two methods than was observed for the symmetrical wicket gate, although the difference is still not extremely large. For the cambered wicket gate the maximum difference is approximately 6°, while for the symmetrical wicket gate the difference is approximately 3.5°. For the cambered wicket gates the potential flow solution is expected to yield the more accurate results, since it can account for the details of the wicket gate shape. This conclusion is mostly speculation, however, and cambered wicket gates should be studied experimentally in the future. One advantage of the potential flow solution is that stay vanes can be added to the analysis for cases where the gate spacing is such that inlet conditions to the gates will affect the exit flow angle. The pressure distribution on the wicket gates can also be obtained from the potential flow solution, from which the force and moment coefficients for the spindle can be calculated.

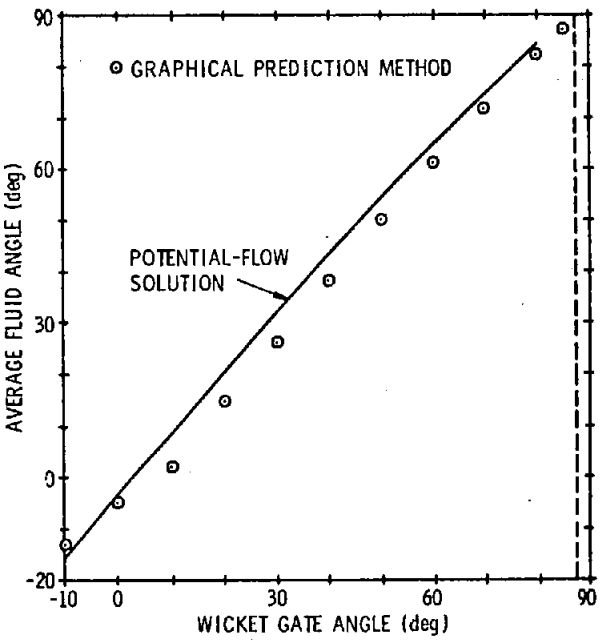

Figure 16. — Comparison of the fluid exit angles predicted for the cambered wicket gate system using the potential flow solution and the graphical approach.

Before concluding this section on the theoretical and experimental results, an additional comparison is made between the local fluid angles measured and the fluid angles predicted at the probe radius for the symmetrical wicket gate. Only the potential flow solution is capable of calculating the local flow properties, and the comparison of the flow angle distributions is made to demonstrate these capabilities. Figure 17 presents the flow angles predicted and measured downstream of several wicket gate passages. The positive direction of the circumferential location coordinate is in the same direction as the mean swirl of the flow and opposite to the positive θ direction shown on figure 12. In general, figure 17 shows that the predicted and measured data have the same trends and that the slope of data is almost identical. The mean value of the two sets of data is the main difference, which tends to make the prediction look worse than it is. The mean values only differ by approximately 2°. It should be pointed out that the large extreme angles in the experimental data are erroneous measurements made with the probe in the wake of wicket gates. Eliminating these points would make the prediction appear more accurate.

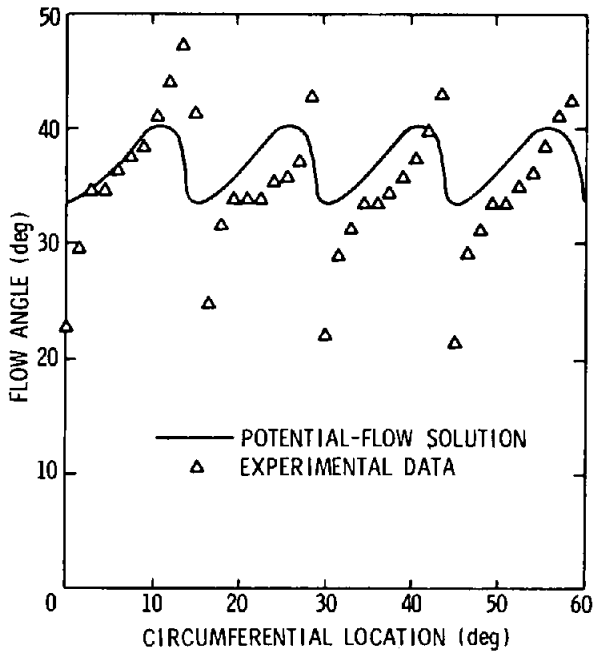

Figure 17. — Local fluid angle versus circumferential location measured downstream of the wicket gates and predicted by the potential flow solution.

BIBLIOGRAPHY

[1] Falvey, H. T., "Draft Tube Surges — A Review of Present Knowledge and an Annotated Bibliography," Bur. Reclam., Rep. REC-ERC-71-42, December 1971.

[2] Cassidy, J. J., "Experimental Study and Analysis of Draft-Tube Surging," Bur. Reclam., Rep. REC-OCE-69-5, October 1969.

[3] Palde, U. J., "Model and Prototype Turbine Draft Tube Surge Analysis by the Swirl Momentum Method," IAHR and Symposium, 1974.

[4] Palde, U. J., "Influence of Draft Tube Shape on Surging Characteristics of Reaction Turbines," Bur. Reclam. Rep. REC-ERC-72-24, July 1972.

[5] Falvey, H. T. and J. J. Cassidy, "Frequency and Amplitude of Pressure Surges Generated by Swirling Flow," Trans. Symposium International Association for Hydraulic Research, pt 1, Paper El, Stockholm, Sweden, 1970.

[6] Cassidy, J. J. and H. T. Falvey, "Observations of Unsteady Flow Arising After Vortex Breakdown," J. Fluid Mech., vol. 41, pt 4, pp. 727-736, 1970.

[7] Giesing, J. P., "Extensions of the Douglas Neumann Program to Problems of Lifting, Infinite Cascades," U. S. Dep. Commerce Rep. LB 31653, AD 605207, revised July 2, 1964.

APPENDIX A

Appendix A

Results of Preliminary Tests Indicating Effect of Test Apparatus Geometry on Surge Pressure

The test facility for the draft tube surge study as shown in Figure 3 was not the original test apparatus considered in the program. The original draft tube surge test facility was designed, fabricated, and assembled as shown in Figure 14*. The main difference between the original test facility and the one finally used for testing is the location of the air supply flow fan. In the original test facility, (Figure 14), air was drawn from the open atmosphere into the test section and dumped into a stilling chamber by means of a flow fan downstream of the draft tube. In the final test facility, (Figure 3)*, air was blown into a stilling chamber first, then passed through the test section and dumped to atmosphere.

Examination of the sketches of the two facilities would seem to indicate that the important flow characteristics (pressure parameter and frequency parameter) produced in either test facility would be essentially the same. The authors felt that it was important for the test facility to produce relations between the surge parameters and the momentum parameter similar to those obtained by Palde [4]. Preliminary tests in the original test apparatus provided a relation between frequency parameter and momentum parameter much like that obtained by Palde. However, pressure parameter as a function of momentum parameter was essentially constant, which radically disagreed with Palde's data. In an attempt to obtain pressure parameter data similar to Palde's, various pressure pick-up devices were tried at various locations along the draft tube. After repeated failure to obtain the desired data in the original test facility, a test facility similar to that used by Palde (i.e., pushing air through the draft tube and dumping to atmosphere) was constructed as shown in Figure 3. Surging characteristics obtained in the modified test facility agreed very well with Palde's data. The altered test facility solved the problem but raised a question. Why was the pressure parameter much lower for the original test facility compared to that obtained in Palde's or the final test facility? Velocity profiles obtained in the draft tube at L/D=4.40 for each facility at various momentum parameters were compared. Figure A.1 shows that the velocity profiles are quite similar for both test facilities.

In an effort to answer this question a brief series of tests were performed to investigate the effects on pressure parameter of dumping the draft tube flow into a stilling chamber and then dumping to atmosphere. Tests were performed on both the cylindrical and elbow type draft tubes. Tables A.1 and A.2 show the different geometries that were investigated. With any given facility geometry tested, a survey of pressure parameter as a function of momentum parameter was obtained. The flowrate through the test facility was measured by an orifice meter and the surge pressure was measured through a dynamically calibrated pressure transducer by an RMS meter as earlier described in this report.

*Refers to the figures in the text

Table A.1

1. STILLING CHAMBER AND AIR SUPPLY DOWNSTREAM OF DRAFT TUBE

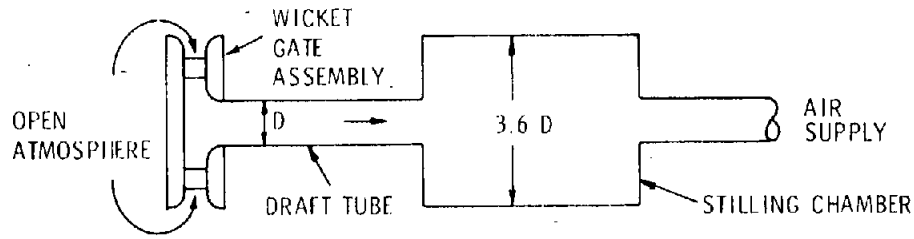

2. NO STILLING CHAMBER, UPSTREAM AIR SUPPLY

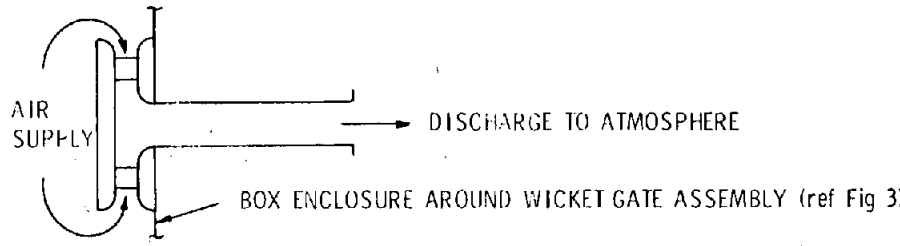

3. STILLING CHAMBER DOWNSTREAM OF DRAFT TUBE, UPSTREAM AIR SUPPLY

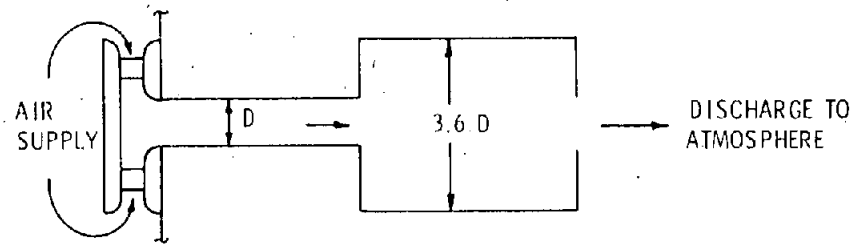

4. STILLING CHAMBER AND AIR SUPPLY UPSTREAM OF DRAFT TUBE

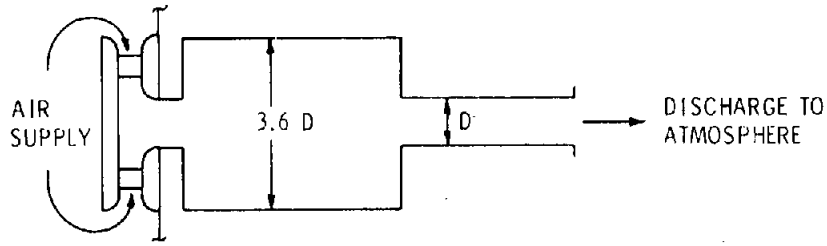

5. STILLING CHAMBER WITH SCREEN DOWNSTREAM OF DRAFT TUBE, UPSTREAM AIR SUPPLY

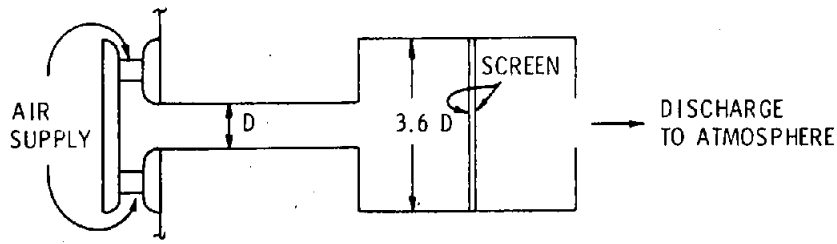

Table A.2

1. NO STILLING CHAMBER, UPSTREAM AIR SUPPLY

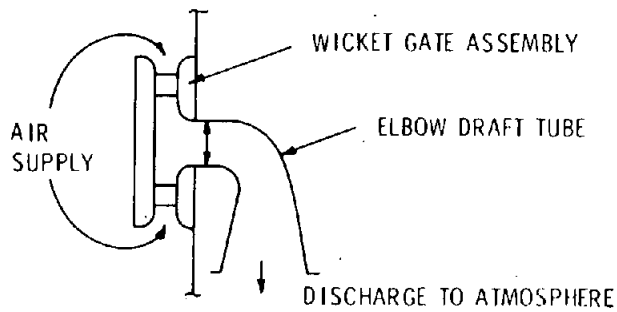

2. STILLING CHAMBER DOWNSTREAM OF DRAFT TUBE, UPSTREAM AIR SUPPLY

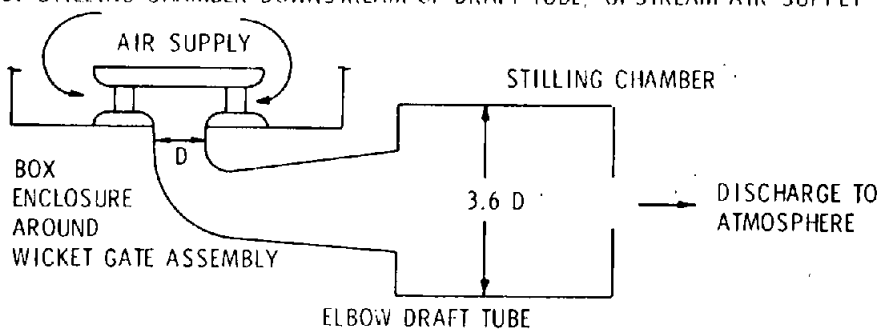

3. STILLING CHAMBER (SHORT CONNECTION) UPSTREAM OF DRAFT TUBE, UPSTREAM AIR SUPPLY

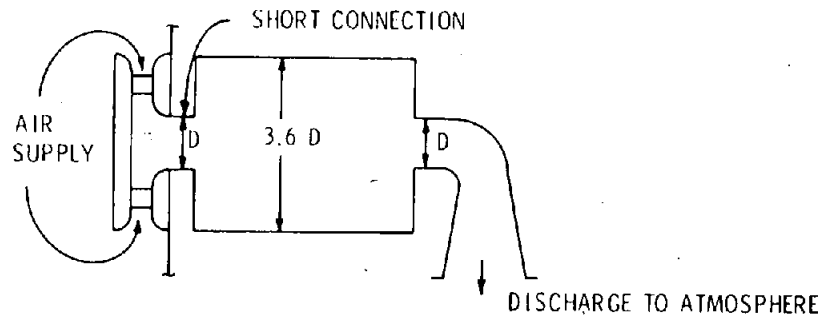

4. STILLING CHAMBER (LONG CONNECTION) UPSTREAM OF DRAFT TUBE, UPSTREAM AIR SUPPLY

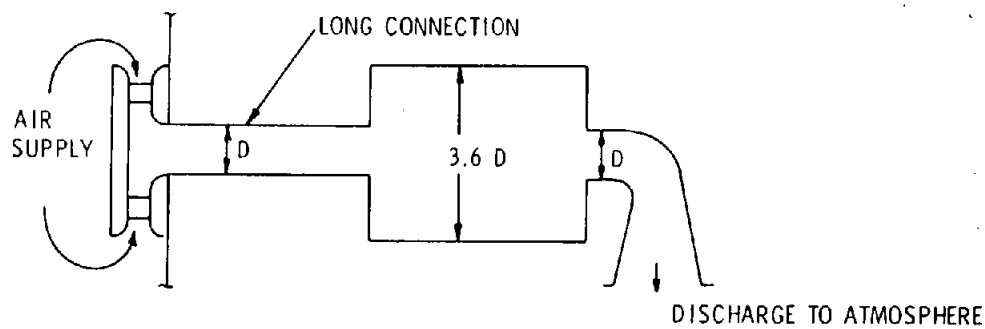

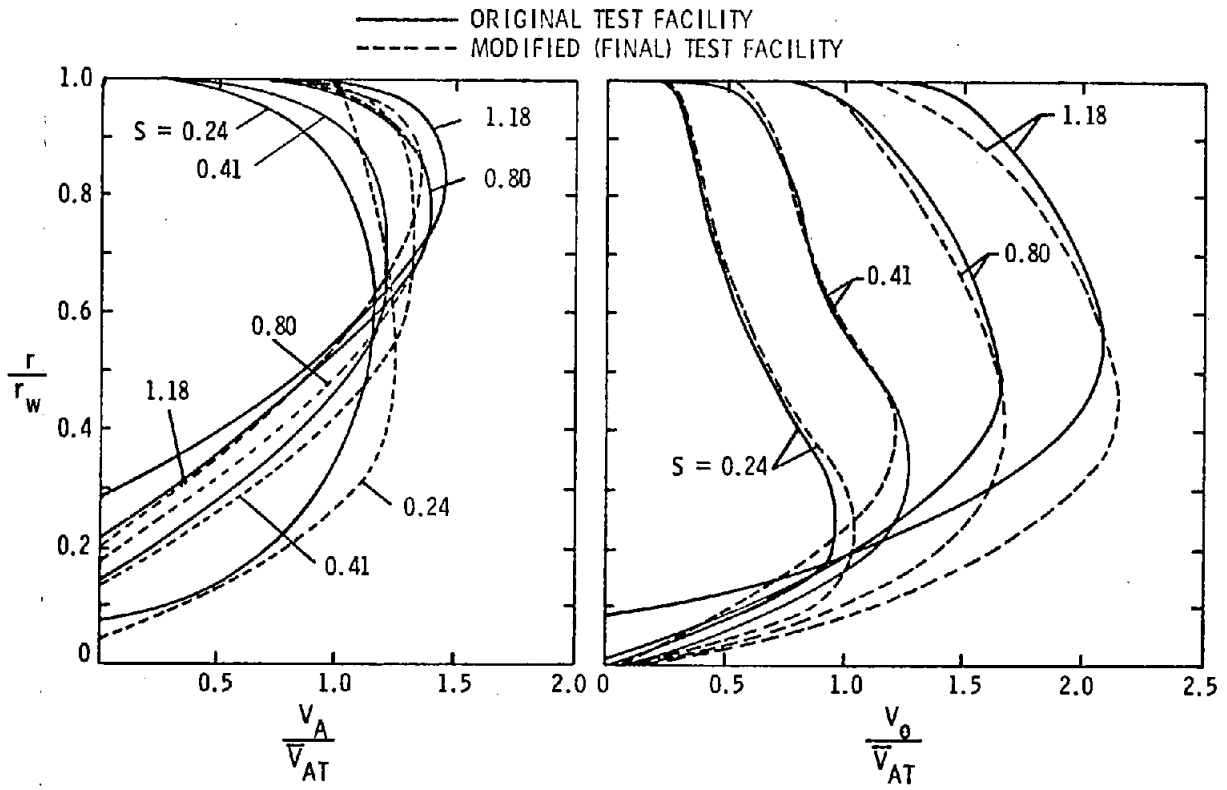

Figure A.1 - Axial and Tangential Velocities in the Original and Modified Test Facility

Figure A.2 shows the results of this investigation for the cylindrical draft tube and likewise, Figure A.3 corresponds to the Fontenelle (elbow type) draft tube. The numbers on the curves in Figures A.2 and A.3 correspond to the geometries so numbered in Tables A.1 and A.2. Comparison of curves (1) and (2) in Figure A.2 shows the effects of a stilling chamber below the draft tube on pressure parameter. Looking at all the curves of both Figures A.2 and A.3, it is obvious that the use of the stilling chamber in all cases reduced the pressure parameter magnitude. Notice that screens placed across the stilling chamber (curve (5), Figure A.2) forced the pressure parameter relation of the original test facility to become almost identical to those of Palde and curve (2).

Out of this brief study comes speculation that stilling chambers placed downstream of a turbine runner may be an effective means of reducing draft tube surge in hydroelectric pump-turbines. Further study is required in this area.

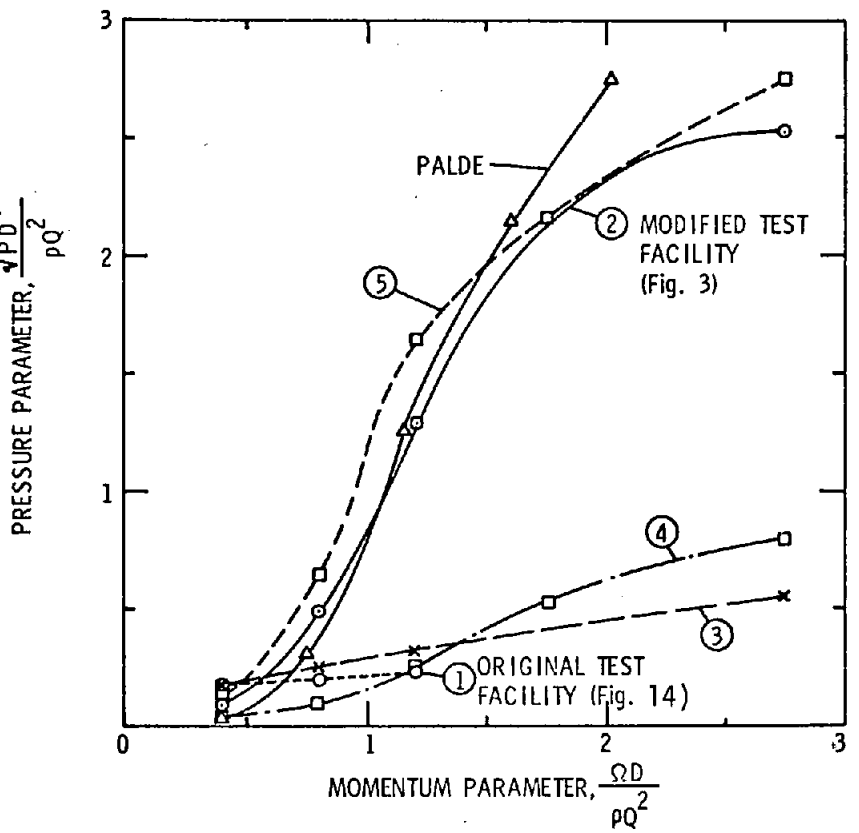

Figure A.2 - Pressure versus Momentum Parameter for the Cylindrical Draft Tube as a Function of Test Facility Geometry

A second complication has been suggested by H. Falvey of The Bureau of Reclamation. This involves the geometry of model test loops which have stilling chambers located up or downstream of model pump-turbines. The water level and geometry of these chambers could provide surge characteristics, based on model tests, that are inconsistent with those of the prototype.

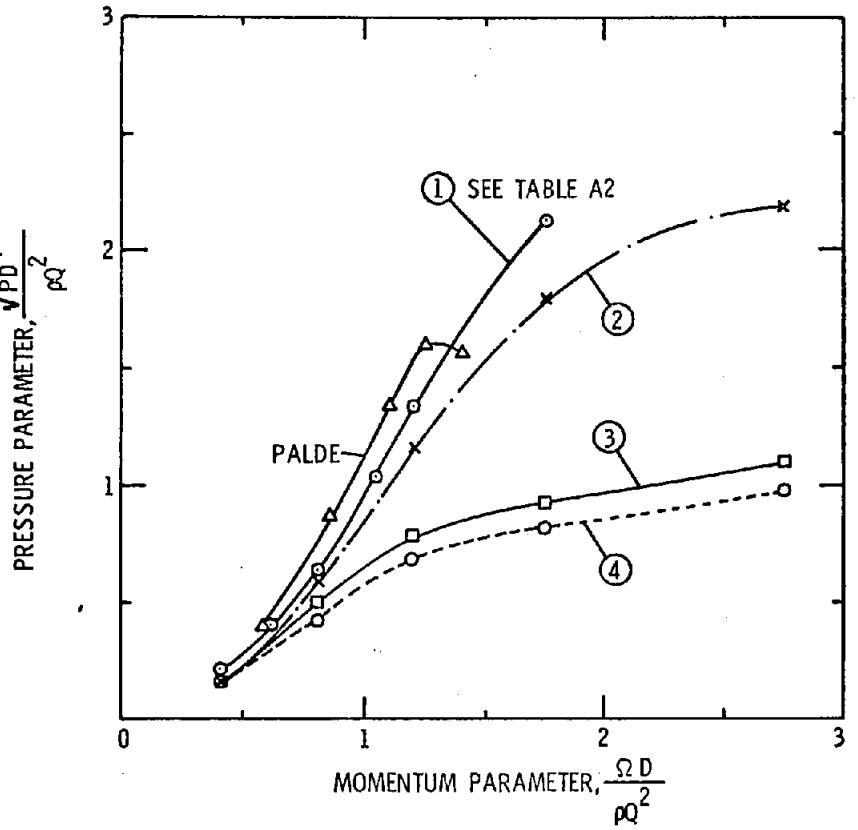

Figure A.3 - Pressure versus Momentum Parameter for the Fontenelle (Elbow Type) Draft Tube as a Function of Test Facility Geometry

APPENDIX B

Appendix B

Description of the Computer Code to Solve the Flow Field Through the Wicket Gates and a Sample Problem

Introduction

The purpose behind the development of the following computer program was to obtain a fast and accurate means of determining the fluid exit angle from the wicket gates of a hydraulic turbine. This information was needed as an aid in the prediction of draft tube surge. It was felt that an analysis of the actual flow field through the wicket gates would be required to obtain a solution with improvements over the currently employed graphical approach. The details of the techniques employed are described in Section 3 of the main body of this report. The input to the program was to be the wicket gate geometry and the inlet flow conditions, and the primary desired output, as previously mentioned, was the fluid exit angle. These requirements were easily met. However, with the Douglas-Neumann program used to obtain a potential flow solution in a transformed cascade, additional output, such as the pressure distribution on the wicket gates, force and moment coefficients for the wicket gate spindles, and local velocities at points off the body were also obtained.

The major portion of the computer code consists of the original Douglas-Neumann cascade program which is documented in Reference [7]. The input was modified to accommodate the geometry of the wicket gate system. Since the Douglas-Neumann cascade program is a generalized program, numerous control codes could also be set constant internally because they did not apply to the type of solution under consideration. With the geometry of the wicket gate system as input to the program, a section was then added which transformed the original geometry into a rectangular cascade in the required form for the Douglas-Neumann solution. The solution then provides the flow exit angle, local velocities at the midpoints of the segments on the airfoil, and, if desired, velocity components at points off the body. The modification to the exit angle consisted of only a change in the sign, which was necessary to coincide with the convention adopted for the wicket gate system. The velocities on the airfoil surface and the off-body point velocities were transformed back to the original plane using the equations of Section 3.4. Integration of the pressure distribution, which was obtained from the known velocities at the segment midpoints, yielded the desired force and moment coefficients for the wicket gate spindle.

Description of Input and Output

Input

The input to the program and the various options available when running the program will be defined as each required input card is described. Figure B.1, which has an enlarged schematic of a single

wicket gate and a schematic of the radial cascade of wicket gates, defines all of the geometric parameters involved and the sign conventions used. The x and y coordinate system drawn on the wicket gate at $\theta=0$ also shows how the wicket gate coordinates relate to the radial cascade.

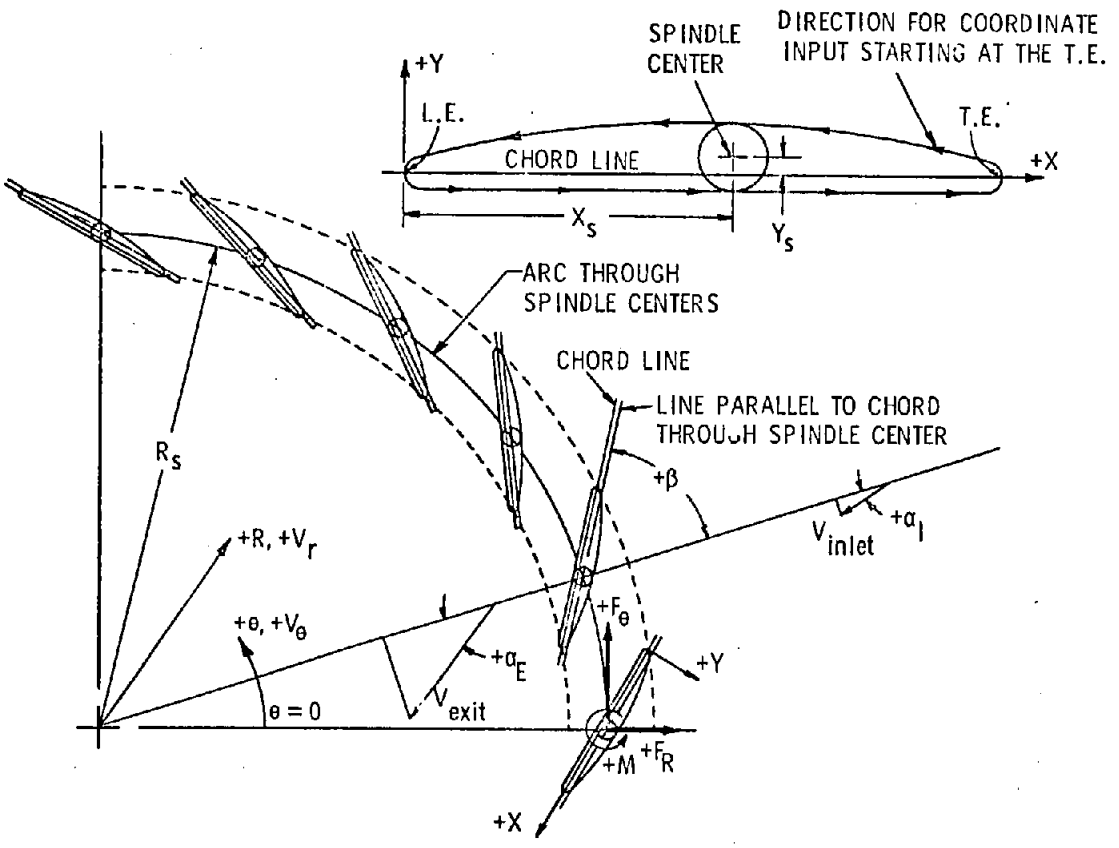

Figure B.1 - Schematic of a Wicket Gate and the Cascade of Wicket Gates Describing the Program Input and Output Parameters

The following set of input cards are required by the program. These sets can be repeated numerous times with the program continuing to process additional runs until terminated by an input code.

CARD 1 Heading Card

The first card is simply a heading card, which can be punched with any desired heading describing the run. This heading will appear at the top of each page of printed output. The entire card can be used. FORMAT(20A4)

CARD 2 Run Control Card

From this card, values for the following four integer variables are read:

FLGO2 FLGO8 FLGO9 FLG12 FORMAT(4I1)

These parameters control the various options available in the program.

FLGO2 FLGO2 is a nonzero integer if the flow is to be determined at points off the body.

FLGO8 As described in Section 3.3 of the main body of this report, the Douglas-Neumann program obtains a particular solution by combining 3 basic solutions. If the wicket gate geometry of the current run is identical to the previous run (i.e., only the flow inlet angle is changed), the three basic solutions need not be computed again, but the program can go directly to obtaining a new solution from the basic solutions. FLGO8 is input as a nonzero integer to direct the program to go directly to the combination solution. If FLGO8 is nonzero, cards 3 and 4 are still necessary.

FLGO9 If the flow is to be determined at points off the body, the coordinates of these points can be read into the program or calculated internally. Giving FLGO9 a nonzero value directs the program to use the remaining number of available points (100 - number of body coordinates) and calculate coordinates equally spaced across one wicket gate sector at a specified constant radius. The first point is at $\theta=0$ and the last point occupies a similar position with respect to the next wicket gate. The radius for these points, ROFFB, is punched on a subsequent card. This option can only be used at radii upstream or downstream of the wicket gate leading and trailing edges, respectively.

FLG12 The program will attempt to continually process additional runs until FLG12 is input as a nonzero integer. Termination of the program, thus, requires a heading card, which can be left blank, and a run control card with a nonzero integer punched in column 4.

CARD 3 Body Coordinate Control Card

Card 3 and a similar card used for the off-body coordinates supply the program with data concerning the coordinates. The values for the following variables are punched on card 3.

NN BDN SUBKS ROFFB FORMAT(I5,3X,2I1,F10.0)

NN NN is the number of coordinates, which for this card is the number of body coordinates. The total number of body coordinates and off-body coordinates is 100. NN must be right justified in column 5.

BDN BDN is an integer variable which tells the program whether body coordinates or off-body coordinates are to follow. For card 3, BDN must be nonzero.

SUBKS SUBKS is an integer variable punched in column 10 which for card 3 gives the option of using the X and Y body coordinates from the previous case. SUBKS is given a nonzero value to use the previous coordinates, thus eliminating the need for duplicate decks of body coordinates. None of the other geometric variables need to be the same to apply this option.

ROFFB ROFFB is the radius for the off-body points when calculating the coordinates internally. Although ROFFB appears in the same READ statement as the 3 previous parameters, it need not be specified at this time.

CARD 4 System Geometric Data

Values for the following parameters are punched on card 4 with the given format.

NLE NWG WGA FALPHR RS XS YS FORMAT(2I5,5F10.0)

NLE Coordinates for the body are read into the program in a counter clockwise direction starting at the trailing edge. This direction is indicated on the enlarged sketch of the wicket gate in Figure B.1. NLE is the number of the coordinate at the leading edge of the wicket gate and is required to identify the leading edge in the transformation. NLE must be right justified in column 5.

NWG NWG is the number of wicket gates in the system. NWG must be right justified in column 10.

The following 5 parameters are each punched in a field of ten columns starting in column 11. A decimal point must be punched.

WGA WGA is the wicket gate angle in degrees which is denoted by β in Figure B.1. The configuration shown in the figure represents a positive angle.

FALPHR FALPHR is the flow inlet angle in degrees denoted by α_I in Figure B.1. The positive direction is indicated in the figure.

RS RS is the radius of the spindle centers expressed in chord lengths.

XS & YS XS and YS are the coordinates of the spindle center with respect to the origin of the cartesian system located at the leading edge of the wicket gate. These values are indicated on the enlarged sketch of the wicket gate in Figure B.1. XS and YS must be expressed in chord lengths.

Coordinate Data FORMAT(2F10.5)

The next NN cards contain the X and Y coordinates of the wicket gate with respect to the cartesian system designated in Figure B.1. Values of X and Y for each point are punched in the first two fields of ten columns on the cards with the decimal point present. These values must be in terms of percent chord. It is also essential that the order of the data starts at the trailing edge, progresses counterclockwise around the wicket gate, and ends at the trailing edge with the first point repeated. The direction for the coordinate input is also indicated in Figure B.1. This set of cards is eliminated if FLG08 is nonzero or if SUBKS is nonzero.

Input for Off-Body Points, if Desired

CARD 1B

Card 1B contains the same parameters for the off-body coordinates as card 3 did for the body coordinates. The values for the following parameters are required:

NN BDN SUBKS ROFFB FORMAT(I5,3X,2I1,F10.0)

NN NN is the number of off-body coordinates. This value must be right justified in column 5. If the off-body coordinates are calculated internally, the value of NN read in is ignored.

BDN For card 1B, BDN must be zero and is punched in column 9.

SUBKS SUBKS has the same function for the off-body points as it had for the body coordinates. SUBKS is a nonzero integer punched in column 10 if the off-body points from the previous case are to be used in the current run.

ROFFB ROFFB is the radius for the off-body points when calculating the coordinates internally. ROFFB

must be expressed in chord lengths and punched in columns 11 through 20 with the decimal present. If the off-body coordinates are not calculated internally, no value needs to be specified for ROFFB.

Off-Body Coordinate Data FORMAT(2F10.5)

The off-body coordinates are read into the program with the same format as the body coordinates. In this case, the coordinates are R and θ, where R is the radius nondimensionalized by the chord and θ is the angular location in degrees. The cards with these coordinates are eliminated if FLG09 or SUBKS are nonzero.

As previously mentioned, the preceding sets of cards can be repeated as often as desired for making multiple runs of different geometries and inlet conditions, until the program is terminated by making FLG12 nonzero. If FLG08 is nonzero, only the first 4 cards are required. The sets of coordinate data can also be eliminated, if they are identical with the previous run, by making SUBKS nonzero. The off-body coordinates are eliminated if FLG09 is nonzero.

Following this description of the input and output is the listing of the computer code. The program is written in FORTRAN and currently uses 6 files on magnetic tape for storage. Following the program listing is a listing of the input for a sample problem with the wicket gate geometry shown in Figure B.1. For this sample problem, WGA=60.0, α_I=60.0 and the off-body coordinates are input from cards.

Output

On the first page of output from the program the input parameters which control the run are listed. These parameters are identified using the nomenclature just defined. Before describing the remaining output, several new coefficients need to be defined. It is recalled from Section 3.4 that v_{r_s} is the normalizing velocity used to nondimensionalize the velocity in the original plane. A pressure coefficient is also formed using v_{r_s} as the normalizing velocity and is defined as follows:

$$C_p = 1 - \left(\frac{v_\ell}{v_{r_s}}\right)^2 = \frac{ps_\ell - ps_{r_s}}{\frac{1}{2}\rho v_{r_s}^2} \qquad \text{(B.1)}$$

where

v_ℓ is the local velocity at a point on the wicket gate

and

ps_ℓ is the local static pressure .

p_{sr_s} is the reference static pressure defined in terms of v_{r_s} and the total pressure, p_T.

$$p_{sr_s} = p_T - \frac{1}{2} \rho v_{r_s}^2 \quad . \tag{B.2}$$

The flow field solution yields the dimensionless local velocity and the pressure coefficient at the midpoint of each segment defining the body. Using the pressure distribution on the wicket gate, the force components (F_θ and F_R) and the moment (M) acting on the spindle can easily be calculated. The positive sign convention for the forces and moment are indicated on the wicket gate at θ=0 in Figure B.1. Three coefficients are defined which represent F_θ, F_R and M in dimensionless terms.

$$C_{F_\theta} = \frac{F_\theta}{\frac{1}{2} \rho v_{r_s}^2 cB} \tag{B.3}$$

$$C_{F_R} = \frac{F_R}{\frac{1}{2} \rho v_{r_s}^2 cB} \tag{B.4}$$

$$C_M = \frac{M}{\frac{1}{2} \rho v_{r_s}^2 c^2 B} \tag{B.5}$$

With the definitions of the preceding three coefficients and the pressure coefficient, all of the output parameters have been defined and are easily identified on the computer output. At the top of each page of output for the on-body data, the descriptive data is printed, the flow inlet and exit angles are given, and values for the three coefficients are given. Following these data are the original body coordinates in percent chord, and between the original coordinates are the coordinates of the midpoints of the segments. Directly over from the midpoint coordinates is the dimensionless velocity and the pressure coefficient calculated for that segment midpoint. The off-body data is the last part of the output, giving the R and θ coordinates and the two dimensionless velocity components for the off-body points. A sample output for the case previously mentioned in the input section is presented following the listing of the input data. A plot of the pressure distribution computed for this sample problem is presented in Figure B.2 for an indication of the type of results obtained.

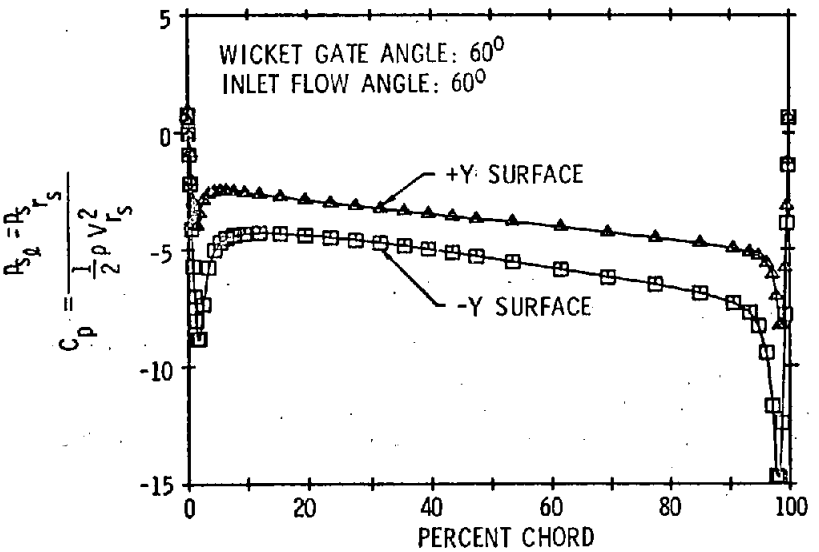

Figure B.2 - Sample Pressure Distribution for the Cambered Wicket Gate

PROGRAM LISTING

```
//              'P3497,T=300,R=30000,S=280,4600','DAVIS R F'
/*FULLSKIPS
// EXEC SETTAF,FORMS=16,TRAIN=TN
// EXEC FWCG,PARM=NOCMPRS
//SYSIN DD *
      COMMON IM,NER,NT,NB,NCFLG,RPI,R2PI,SP,CL,ALPHA,FALPHA
     1,DALFA,CHORD,FLG02,FLG03,FLG04,FLG05,FLG06,FLG07,FLG08,FLG09,
     2FLG10,FLG11,FLG12,ND,NLF,SUMDS,XS,YS,RS,WGA,NWG
      DIMENSION ND(10),NLF(10),SUMDS(10)
      COMMON/BLK1/HEDR(20),THETA
      COMMON/BLK2/ Z(100),Q(100),SINA(100),COSA(100)
      COMMON/BLK3/ X(100),Y(100),XMP(100),YMP(100),R(100)
      COMPLEX IM,Z,Q
      INTEGER FLG02,FLG03,FLG04,FLG05,FLG06,FLG07,FLG08,FLG09,
     -FLG10,FLG11,FLG12
   10 CALL PART1
      IF(FLG08 .NE. 0) GO TO 60
      CALL PART2
   20 CALL PART4
   30 CALL PART5
   60 CALL PART6
      GO TO 10
      END
```

```
      SUBROUTINE PART1
      COMMON IM,NER,NT,NB,NCFLG,RPI,R2PI,SP,CL,ALPHA,FALPHA
     1,DALFA,CHORD,FLG02,FLG03,FLG04,FLG05,FLG06,FLG07,FLG08,FLG09,
     2FLG10,FLG11,FLG12,ND,NLF,SUMDS,XS,YS,RS,WGA,NWG
      COMMON/BLK1/HEDR(20),THETA
      COMMON/BLK2/ Z(100),Q(100),SINA(100),COSA(100)
      COMMON/BLK3/ X(100),Y(100),XMP(100),YMP(100),R(100)
      DIMENSION DELS(100),ND(10),NLF(10),SUMDS(10)
      COMPLEX IM,Z,Q
      INTEGER BDN,SUBKS
      INTEGER FLG02,FLG03,FLG04,FLG05,FLG06,FLG07,FLG08,FLG09,
     -FLG10,FLG11,FLG12
      PI=3.141593
      IM=(0.0,1.0)
      READ (5,700) (HEDR(I),I=1,20)
  700 FORMAT (20A4)
      WRITE(6,601)
  601 FORMAT('1',10X,'INPUT PARAMETERS'/)
      READ(5,4)FLG02,FLG08,FLG09,FLG12
    4 FORMAT(4I1)
C     FLG02 IS NONZERO IF FLOW IS TO BE DETERMINED AT POINTS OFF THE BODY
C     FLG08 IS NONZERO TO GO DIRECTLY TO THE COMBINATION SOLUTIONS OF
C       THE PREVIOUS CASE. THIS FLAG CAN ONLY BE USED IF THE WICKET
C       GATE GEOMETRY IS UNCHANGED, IE, ONLY THE FLOW INLET ANGLE
C       IS CHANGED.
C     FLG09 IS NONZERO IF OFF-BODY COORDINATES ARE CALCULATED INTERNALLY.
C     FLG12 IS NONZERO TO TERMINATE THE PROGRAM
      WRITE(6,602)FLG02,FLG08,FLG09,FLG12
  602 FORMAT(' ',13X,'FLG02 = ',I1/14X,'FLG08 = ',I1/14X,'FLG09 = ',I1/
     114X,'FLG12 = ',I1)
C     NB = NUMBER OF CASCADES, NB GT 1 WAS USED IN ORIGINAL DN PROGRAM
C     FOR INTERACTION PROBLEMS
      NB=1
C     FLG03 THRU FLG07 ARE CONTROL CODES USED IN ORIGINAL DN PROGRAM
      FLG03=0
      FLG04=0
      FLG05=1
      FLG06=0
      FLG07=0
C     FLG10 AND FLG11 ARE NOT USED
      FLG10=0
      FLG11=0
      DALFA=0.0
      IF(FLG12.NE.0)GO TO 920
      GO TO 80
  920 WRITE(6,930)
  930 FORMAT(1X,// 1X,'END OF PROGRAM - DATA HAS BEEN EXHAUSTED')
      STOP
   80 IF(FLG08.NE.0)GO TO 121
      NT=0
      NCFLG=2
      REWIND 4
      REWIND 9
```

```
       REWIND 13
       DO 120 I=1,10
       NLF(I)=0.
       SUMDS(I)=0.
  120  ND(I)=0.
  121  CONTINUE
C      K2 = TOTAL NUMBER OF COORDINATES SETS
C      K2 = NUMBER OF BODIES (+1 IF USING OFF-BODY POINTS)
       K2=NB
       IF (FLG02 .NE. 0) K2=NB+1
       ISTR=1
       ISTOP=0
       DO 2000 L=1,K2
       LM1=L-1
C      CL, ALPHA, AND DALFA ARE INPUT PARAMETERS IN THE ORIGINAL
C      DN PROGRAM, THEY ARE NOT USED IN THIS PROGRAM
       CL=0.0
       ALPHA=0.0
       DALPHA=0.0
       READ(5,15)NN,BDN,SUBKS,ROFFB
   15  FORMAT(I5,3X,2I1,F10.0)
       WRITE(6,603)NN,BDN,SUBKS,ROFFB
  603  FORMAT(' ',13X,'NN = ',I3/14X,'BDN = ',I1/14X,'SUBKS = ',I1/
      114X,'ROFFB = ',F10.7)
       IF(FLG09.NE.0.AND.BDN.EQ.0)NN=100-ND(LM1)
       IF(BDN.NE.0)READ(5,16)NLE,NWG,WGA,FALPHR,RS,XS,YS
   16  FORMAT(2I5,5F10.0)
       IF(BDN.NE.0)WRITE(6,604)NLE,NWG,WGA,FALPHR,RS,XS,YS
  604  FORMAT(' ',13X,'NLE = ',I2/14X,'NWG = ',I2/14X,'WGA = ',F9.5/
      114X,'FALPHA = ',F9.5/14X,'RS = ',F10.7/14X,'XS = ',F10.7/
      214X,'YS = ',F11.7)
       FALPHA=-FALPHR
       IF(FLG08.NE.0)GO TO 9119
C      NLE = NUMBER OF THE LEADING EDGE COORDINATES
C      NWG = NUMBER OF WICKET GATES
C      WGA = WICKET GATE ANGLE ANGLE FROM THE RADIAL POSITION (DEG.)
C      FALPHA = INLET FLOW ANGLE, MEASURED FROM A RADIAL LINE (DEG.)
C      RS = RADIUS OF THE SPINDLE CENTERS (CHORD LENGTHS)
C      XS AND YS ARE SPINDLE COORDINATES (CHORD LENGTHS)
C      ROFFB = RADIUS FOR OFF-BODY POINTS IF COORDINATES ARE CALCULATED
C        INTERNALLY (CHORDS LENGTHS)
C      NN = NUMBER OF COORDINATES TO BE READ IN
C      BDN AND SUBKS ARE CONTROL VARIABLES
C      BDN = 0 IF OFF-BODY COORDINATES FOLLOW
C      BDN IS NONZERO IF BODY COORDINATES FOLLOW
C      SUBKS IS NONZERO TO USE THE UNMODIFIED COORDINATES OF THE BODY OF
C        THE PREVIOUS CASE
       NLFF=0
C      NLFF = PARAMETER IN ORIGINAL DN PROGRAM USED TO MAKE CALCULATIONS
C      FOR NON-LIFTING BODIES
       ND(L)=NN
       NLF(L)=NLFF
       NT=NT+NN
```

```
      IF(L.EQ.1)GO TO 17
      ISTR=ISTR+ND(LM1)
   17 ISTOP=ISTOP+NN
      IST2=ISTR-L+1
      ISTP2=ISTOP-L
      IF(NLEE .EQ. 0) NCFLG = NCFLG+1
      IF( BDN .EQ. 0) NCFLG=NCFLG-1
      IF(SUBKS .EQ. 0) GO TO 140
      READ (13) (X(I),I=ISTR,ISTOP)
      READ (13) (Y(I),I=ISTR,ISTOP)
      IF(BDN.NE.0)GO TO 139
      DO 138 I=ISTR,ISTOP
      Y(I)=Y(I)*PI/180.0
  138 CONTINUE
      GO TO 211
  139 READ(13)(SKIP,I=IST2,ISTP2)
      READ(13)(SKIP,I=IST2,ISTP2)
      GO TO 150
  140 IF(FLG09.NE.0.AND.BDN.EQ.0)GO TO 143
      DO 142 I=ISTR,ISTOP
      READ(5,20) X(I),Y(I)
   20 FORMAT(2F10.5)
  142 CONTINUE
      GO TO 145
  143 RNWG=NWG
      RISTR=ISTR
      RNN=NN
      RNN1=RNN-1.0
      DO 144 I=ISTR,ISTOP
      X(I)=ROFFB
      RI=I
      RI=RI-RISTR
      Y(I)=RI*360.0/RNWG/RNN1
  144 CONTINUE
  145 WRITE(13)(X(I),I=ISTR,ISTOP)
      WRITE (13) (Y(I),I=ISTR,ISTOP)
      IF(BDN.NE.0)GO TO 150
      DO 146 I=ISTR,ISTOP
      Y(I)=Y(I)*PI/180.0
  146 CONTINUE
  150 IF(BDN.EQ.0)GO TO 211
      IF(SUBKS .NE.0) GO TO 200
C     XMP AND YMP ARE THE COORDINATES OF THE MIDPOINTS OF THE SEGMENTS
      DO 160 I=IST2,ISTP2
      XMP(I)=(X(I+1)+X(I))/2.
  160 YMP(I)=(Y(I+1)+Y(I))/2.
      WRITE(13) (XMP(I),I=IST2,ISTP2)
      WRITE(13) (YMP(I),I=IST2,ISTP2)
  200 CONTINUE
      WGAR=WGA*PI/180.0
      CWGA=COS(WGAR)
      SWGA=SIN(WGAR)
      DO 201 I=ISTR,ISTOP
```

```
      X(I)=X(I)/100.0
      Y(I)=Y(I)/100.0
  201 CONTINUE
      DO 210 I=ISTR,ISTOP
C     X AND Y ARE CHANGED SO THAT THE WICKET GATE IS ROTATED
C       WGA DEGREES AND THE TURBINE AXIS IS THE CENTER OF THE
C       COORDINATE SYSTEM
      XT=X(I)
      X(I)=RS+(XS-XT)*CWGA+(Y(I)-YS)*SWGA
      Y(I)=(XS-XT)*SWGA-(Y(I)-YS)*CWGA
C     THE WICKET GATE AT X = RS, Y = 0 IS TRANSFORMED
      XT=X(I)
      R(I)=SQRT(XT**2+Y(I)**2)
      X(I)=ALOG(R(I))
      Y(I)=ATAN(Y(I)/XT)
  210 CONTINUE
C     THE ORIGIN IS TRANSFERED TO THE LEADING EDGE AND +X IS REVERSED
      XLE=X(NLE)
      YLE=Y(NLE)
      GO TO 213
  211 DO 212 I=ISTR,ISTOP
      R(I)=X(I)
      X(I)=ALOG(X(I))
  212 CONTINUE
  213 DO 220 I=ISTR,ISTOP
      X(I)=XLE-X(I)
      Y(I)=Y(I)-YLE
  220 CONTINUE
      IF(BDN.EQ.0)GO TO 221
C     CHORD = THE CHORD OF THE TRANSFORMED BLADES
C     SP = SPACING BETWEEN THE TRANSFORMED BLADES
      H=Y(NLE)-Y(1)
      W=X(1)-X(NLE)
      CHORD=SQRT(H**2+W**2)
      RNWG=NWG
      SP=2.0*PI/RNWG/CHORD
      THETA=ATAN(H/W)
C     THETA = STAGGER ANGLE OF THE TRANSFORMED BLADES
  221 DO 230 I=ISTR,ISTOP
      X(I)=X(I)/CHORD
      Y(I)=Y(I)/CHORD
  230 CONTINUE
      IF(BDN .EQ. 0) GO TO 500
      SUMS=0.0
      DO 400 I=IST2,ISTP2
      T1=X(I+1)-X(I)
      T2=Y(I+1)-Y(I)
      XMP(I)=(X(I+1)+X(I))/2.
      YMP(I)=(Y(I+1)+Y(I))/2.
      TDS=SQRT(T1*T1+T2*T2)
      DELS(I)=TDS
      SUMS=SUMS+TDS
       SUMDS(L)=SUMDS(L)+TDS
```

```
      COSA(I)=T1/TDS
      SINA(I)=T2/TDS
      Z(I)=CMPLX(XMP(I),YMP(I))
  400 Q(I)=CMPLX(X(I),Y(I))
      Q(ISTOP)=CMPLX(X(ISTOP),Y(ISTOP))
      GO TO 600
  500 IS3=ISTP2+1
      DO 550 I=IST2,IS3
      IP1=I+1
  550 Z(I)=CMPLX(X(IP1),Y(IP1))
  600 CONTINUE
      I2=ISTP2
      IF(BDN.EQ.0)I2=I2+1
      WRITE (9) (Z(I),I=IST2,I2)
      IF(BDN .EQ. 0) GO TO 200
      WRITE(9) (SINA(I),I=IST2,ISTP2)
      WRITE(4) (SINA(I),I=IST2,ISTP2)
      WRITE(9) (COSA(I),I=IST2,ISTP2)
      WRITE(4) (COSA(I),I=IST2,ISTP2)
      WRITE(9) (Q(I),I=ISTR,ISTOP)
 2000 CONTINUE
      NT=NT- NB-ND(NB+1)
C     NT = TOTAL NO. OF ELEMENTS
 9119 RETURN
      END
      SUBROUTINE PART2
      COMMON IM,NER,NT,NB,NCFLG,RPI,R2PI,SP,CL,ALPHA,FALPHA
     1,DALFA,CHORD,FLG02,FLG03,FLG04,FLG05,FLG06,FLG07,FLG08,FLG09,
     2FLG10,FLG11,FLG12,ND,NLF,SUMDS,XS,YS,RS,WGA,NWG
      COMMON/BLK1/HEDR(20),THETA
      INTEGER FLG02,FLG03,FLG04,FLG05,FLG06,FLG07,FLG08,FLG09,
     -FLG10,FLG11,FLG12
      COMMON/BLK2/ Z(100),Q(100),SINA(100),COSA(100)
      DIMENSION   ND(10),A(100),B(100),SUMDS(10),NLF(10),VNS(1000),
     -  VTS(1000)
      COMPLEX IM,Z,Q,W1,W2,TF,T2,T1,CLOG,CSINH
      RPI=0.318309
      R2PI=0.159154
      REWIND 9
      REWIND 10
      REWIND11
      M=1
      N=ND(1)-1
      M1=1
      N1=ND(1)
      DO 100 L=1,NB
      READ(9) (Z(I),I=M,N)
      READ(9) (SINA(I),I=M,N)
      READ(9) (COSA(I),I=M,N)
      READ(9) (Q(I),I=M1,N1)
      M=N+1
      N=N+ND(L+1)-1
      M1=N1+1
```

```
  100 N1=N1+ND(L+1)
      K=NB*NT
      DO 200 I=1,K
      VNS(I)=0.0
  200 VTS(I)=0.0
      NPFLG=0
      A2=0.0
      B2=0.0
      L=NT
  500 DO 1500 J=1,L
      M1=1
      N1=ND(1)-1
      J1=J-L
      J2=0
      J4=0
      T1=COSA(J)-IM*SINA(J)
      DO 1200 I=1,NB
      J1=J1+L
      J4=J4+1
      TF=CSINH(3.14159*(Z(J)-Q(M1))/SP)
      DO 1000 K=M1,N1
      J2=J2+1
      IF(SP .GT.0.0)GO TO 650
      CALL FORM1 (J,K,J2,Z,Q,SINA,COSA,W1)
      IF(SP .EQ.0.0)GO TO 700
      CALL FORM2 (J,K,J2,Z,Q,SINA,COSA,W2)
      IF(NPFLG .NE. 0) GO TO 550
      T2 = CONJG(W2)*T1
      A2=AIMAG(T2)
      B2=REAL(T2)
      GO TO 720
  550 A2=-AIMAG(W2)
      B2=REAL(W2)
      GO TO 750
  650 CALL SPGTO(J,K,J2,SP,TF,Z,Q,SINA,COSA,W1)
  700 IF(NPFLG .NE. 0) GO TO 750
  720 T2=CONJG(W1)*T1
      A1=AIMAG(T2)
      IF(J .EQ. J2) A1=ABS(A1)
      B1=REAL(T2)
      GO TO 800
  750 A1=-AIMAG(W1)
      B1=REAL(W1)
  800 VNS(J1)=VNS(J1)-B1+B2
      VTS(J1)=VTS(J1)+A1-A2
      A(J2)=A1+A2
 1000 B(J2)=B1+B2
      VNS(J1)=VNS(J1)/SJMDS(J4)
      VTS(J1)=VTS(J1)/SJMDS(J4)
      M1=N1+2
 1200 N1=N1+ND(I+1)
      WRITE(10) (A(I),I=1,NT)
      WRITE(10) (B(I),I=1,NT)
```

```
      IF(FLG07 .EQ. 0) GO TO 1300
    5 FORMAT(1HO 12H   AJK   ROW   I4 //(6F15.8))
      WRITE (6,5) J,(A(I),I=1,NT)
      WRITE (6,10) J,(B(I),I=1,NT)
   10 FORMAT(1HO 12H   BJK   ROW   I4 // (6F15.8))
 1300 IF(NT .LE. 135 .OR. NPFLG .NE. 0 ) GO TO 1500
      WRITE(11) (A(I),I=1,NT)
      WRITE(11) (B(I),I=1,NT)
 1500 CONTINUE
      M=1
      N=L
      DO 2000 J=1,NB
      IF (NLF(J) .NE. 0) GO TO 1800
      WRITE(4) (VNS(I),I=M,N)
      WRITE(4) (VTS(I),I=M,N)
 1800 M=N+1
 2000 N=N+L
      IF (FLG07 .EQ. 0) GO TO 3000
      N=NB*L
      WRITE(6,15) (VNS(I),I=1,N)
      WRITE(6,20) (VTS(I),I=1,N)
   15 FORMAT(1HO/10X 3HVNS /// (6F15.8))
   20 FORMAT(1HO/10X 3HVTS /// (6F15.8))
 3000 IF(FLG02 .EQ. 0 .OR. NPFLG .NE. 0 ) GO TO 9292
      NPFLG=1
      L= ND(NB+1)
      READ(9) (Z(I),I=1,L)
      K=NB*L
      DO 3100 I=1,K
      VNS(I)=0.0
 3100 VTS(I)=0.0
      GO TO 500
 9292 RETURN
      END
      SUBROUTINE PART4
      COMMON IM,NER,NT,NB,NCFLG,RPI,R2PI,SP,CL,ALPHA,FALPHA
     1,DALFA,CHORD,FLG02,FLG03,FLG04,FLG05,FLG06,FLG07,FLG08,FLG09,
     2FLG10,FLG11,FLG12,ND,NLF,SUMDS,XS,YS,RS,WGA,NWG
      COMMON/BLK1/HEDR(20),THETA
      INTEGER FLG02,FLG03,FLG04,FLG05,FLG06,FLG07,FLG08,FLG09,
     -FLG10,FLG11,FLG12
      COMPLEX  IM
      DIMENSION A(135,135),R(135,10),ND(10),NLF(10)
      DIMENSION SUMDS(10)
      REWIND 3
      REWIND 4
      REWIND 10
      M=1
      N=ND(1)-1
      DO 100 K=1,NB
      READ(4) (R(I,1),I=M,N)
      READ (4) (R(I,2),I=M,N)
      M=N+1
```

```
  100 N=N+ND(K+1)-1
C     PRECEEDING READS IN SINES,COSINES,ONSET FLOWS NEXT (IF ANY).
      IF (NCFLG .LE. 2 ) GO TO 180
      DO 150 J=3,NCFLG
      READ (4) (R(I,J),I=1,NT)
  150 READ (4)
  180 DO 200 J=2,NCFLG
      DO 200 I=1,NT
  200 R(I,J)=-R(I,J)
  250 DO 300 I=1,NT
      READ (10) (A(I,J),J=1,NT)
  300 READ (10)
      DET=1.
      CALL MIS1 (A,NT,135,R,NCFLG,NERR,DET)
      IF (NERR .NE. 0 ) WRITE (6,350)
  350 FORMAT ( 1H1 23H MATRIX AJK IS SINGULAR )
      DO 500 J=1,NCFLG
  500 WRITE (3) (R(I,J),I=1,NT)
      RETURN
      END
      SUBROUTINE PART5
      COMMON IM,NER,NT,NB,NCFLG,RPI,R2PI,SP,CL,ALPHA,FALPHA
     1,DALFA,CHORD,FLG02,FLG03,FLG04,FLG05,FLG06,FLG07,FLG08,FLG09,
     2FLG10,FLG11,FLG12,ND,NLF,SUMDS,XS,YS,RS,WGA,NWG
      COMMON/BLK1/HEDR(20),THETA
      COMMON/BLK3/ X(100),Y(100),XMP(100),YMP(100),R(100)
      INTEGER FLG02,FLG03,FLG04,FLG05,FLG06,FLG07,FLG08,FLG09,
     -FLG10,FLG11,FLG12
      COMPLEX IM
      DIMENSION B(100),VT(100,5),SIG(100,5),T(100,5),ND(10)
      DIMENSION NLF(10),SUMDS(10)
      REWIND 3
      REWIND 4
      REWIND 10
      REWIND 11
      M=1
      N=ND(1)-1
      DO 100 K=1,NB
      READ(4) (T(I,2),I=M,N)
      READ(4) (T(I,1),I=M,N)
C     READS IN SINES AND COSINES
      M=N+1
  100 N=N+ND(K+1)-1
      IF (NCFLG .LE. 2 ) GO TO 200
      DO 150 J=3,NCFLG
      READ(4)
  150 READ(4) (T(I,J),I=1,NT)
  200 DO 250 J=1,NCFLG
  250 READ(3) (SIG(I,J),I=1,NT)
      DO 400 I=1,NT
      READ(10)
      READ(10) (B(L),L=1,NT)
      DO 400 J=1,NCFLG
```

```
      PR=0.0
      DO 300 L=1,NT
  300 PR=PR+B(L)*SIG(L,J)
  400 VT(I,J)=PR+T(I,J)
      DO 500 J=1,NCFLG
  500 WRITE(11) (VT(I,J),I=1,NT)
      RETURN
      END
      SUBROUTINE PART6
      COMMON IM,NER,NT,NB,NCFLG,RPI,R2PI,SP,CL,ALPHA,FALPHA
     1, DALFA,CHORD,FLG02,FLG03,FLG04,FLG05,FLG06,FLG07,FLG08,FLG09,
     2FLG10,FLG11,FLG12,ND,NLF,SUMDS,XS,YS,RS,WGA,NWG
      COMMON/BLK1/HEDR(20),THETA
      COMMON/BLK2/ Z(100),Q(100),SINA(100),COSA(100)
      COMMON/BLK3/ X(100),Y(100),XMP(100),YMP(100),R(100)
      COMPLEX IM,Z,Q
      INTEGER FLG02,FLG03,FLG04,FLG05,FLG06,FLG07,FLG08,FLG09,
     -FLG10,FLG11,FLG12
      DIMENSION VC(100),CP(100),ND(10),NLF(10),
     1SUMDS(10),GAM(9),DVT(9,10),DV(9,9),SIGT(100),
     3XTEMP(1000),YTEMP(1000),VXL(100),VYL(100),XIJ(100),YIJ(100),DVA(9,
     48),DVX(9,10),ZTEMP(100)
      EQUIVALENCE  (GAM,DVT), (DV,DVT(10)), (DVA,DVT(19))
     1, (VXL,XMP),(VYL,YMP),(XIJ,SINA),(YIJ,COSA)
     2,(ZTEMP,XTEMP(200))
      PI=3.141593
      IF(FLG08 .EQ. 0 ) GO TO 40
      IF(FLG02 .EQ. 0) GO TO 40
      REWIND 10
      J=2*NT
      DO 30 I=1,J
   30 READ (10)
C ** LOOP SKIPS BOTH ON-BODY MATRICES
   40 NER=0
      DET=1.
      K=NCFLG-2
      REWIND 3
      REWIND 4
      REWIND 11
      REWIND 13
      DO 50  J=1,10
      DO 50 I=1,9
      DVX(I,J)=0.0
50    DVT(I,J)=0.0
      IF(FLG03 .EQ. 0 .AND. FLG04 .EQ. 0 .AND. FLG06 .EQ. 0) GO TO 1000
      IF (FLG04 .NE. 0) ALPHA=DALFA
      IF(FLG06 .NE. 0) ALPHA=0.0
      ALPHA=ALPHA/57.29578
      CSALF=COS(ALPHA )
      SNALF=SIN(ALPHA)
      READ(11) (XTEMP(I),I=1,NT)
      READ(11) (YTEMP(I),I=1,NT)
      M=1
```

```
      N=ND(1)-1
      DO 100 I=1,NB
      GAM(I)=(XTEMP(M)+XTEMP(N))*CSALF
      GAM(I)=-(GAM(I)+(YTEMP(M)+YTEMP(N))*SNALF)
      M=N+1
  100 N=N+ND(I+1)-1
      IF(K .EQ.0) GO TO 160
      DO 150 J=1,K
      READ (11) (ZTEMP(I),I=1,NT)
      M=1
      N=ND(1)-1
      DO 150 I=1,NB
      DVA(I,J)= ZTEMP(M)+ZTEMP(N)
      DVX(I,J)= DVA(I,J)
      M=N+1
  150 N=N+ND(I+1)-1
  160 REWIND 11
      IF( K .EQ. NB) GO TO 200
      M=NCFLG-1
      DO 170 I=M,NB
      DVA(I,I)=1.0
  170 DVX(I,I)=1.
  200 CALL MISS (DVA,NB,9,GAM,1,NER,DET)
      IF ( NER .NE. 0 ) WRITE (6,210)
  210 FORMAT (1H1 38HCOMBINATION PROGRAM MATRIX IS SINGULAR )
      IF (FLG03 .NE. 0) GO TO 5000
      IF (FLG06 .NE. 0) GO TO 2000
      DALFA=DALFA/57.29578
      T=0.
      DO 220 I=1,K
  220 T=T+GAM(I)
      T=.5*T/SP
      DAL1=ATAN2(2.0*T*CSALF,1.0-T*T)
      IF( ABS(DAL1-DALFA) .LT. .0005) GO TO 420
      ALF1=ALPHA
      ALF2= ALF1+2.*(DALFA-DAL1)
      ITER=0
  250 CSALF=COS(ALF2)
      SNALF=SIN(ALF2)
      M=1
      N=ND(1)-1
      DO 300 I=1,NB
      GAM(I)=(XTEMP(M)+XTEMP(N))*CSALF
      GAM(I)=-(GAM(I)+(YTEMP(M)+YTEMP(N))*SNALF)
      M=N+1
  300 N=N+ND(I+1)-1
      DO 320 I=1,NB
      DO 320 J=1,NB
  320 DVA(I,J)=DVX(I,J)
      DET=1.
      CALL MISS (DVA,NB,9,GAM,1,NER,DET)
      IF (NER .NE. 0 )WRITE (6,210)
      T=0.0
```

```
      DO 350 I=1,K
  350 T=T+GAM(I)
      T=.5*T/SP
      DAL2=ATAN2(2.*T*CSALF, 1.-T*T)
      IF ( ABS(DAL2-DALFA) .GE. .0005)  GO TO 450
  400 ALPHA=ALF2
  420 DALFA=DALFA*57.29578
      GO TO 5000
  450 ITER=ITER+1
      IF (ITER .LT. 20) GO TO 550
      WRITE(6,500)
  500 FORMAT(1H1,65HALPHA COMPUTATION ITERATIONS EXCEED 20. LAST VALUE O
     -F ALPHA USED. )
      GO TO 400
  550 T=ALF1*(DAL2-DALFA)/(DAL2-DAL1)+ALF2*(DALFA-DAL1)/(DAL2-DAL1)
      ALF1=ALF2
      ALF2=T
      DAL1=DAL2
      GO TO 250
 1000 IF ( FLG05 .NE. 0 ) GO TO 1005
      WRITE(6,1002)
 1002 FORMAT(1H1,30HFLAGS 3, 4, 5, AND 6 ARE ZERO. //
     1 36H COMBINATION PROGRAM CANNOT PROCEED. )
      RETURN
 1005 IF ( FALPHA .NE. 90.0 .AND. FALPHA .NE. 270. ) GO TO 1020
      WRITE(6, 1010)
 1010 FORMAT(1H1 33H UNALLOWABLE INLET ALPHA IS INPUT )
      RETURN
 1020 FALPHA=FALPHA/57.29578
      TNA=SIN(FALPHA)/COS(FALPHA)
      DO 1040 J=1,NCFLG
      READ(11) (XTEMP(I ),I=1,NT)
      M=1
      N=ND(1)-1
      DO 1040 I=1,NB
      DVT(I,J)=XTEMP(N)+XTEMP(M)
      M=N+1
 1040 N=N+ND(I+1)-1
      REWIND 11
      I=NB+1
      DVT(I,1) =-TNA
      DVT(I,2)=1.
      IF( K .EQ. 0 ) GO TO 1120
      F=.5/SP
      DO 1100 J=3,NCFLG
 1100 DVT(I,J) =F
 1120 DO 1140 J=1,I
 1140 GAM(J) = -GAM(J)
      IF ( K .EQ. NB) GO TO 1200
      DO 1160 J= NCFLG,I
 1160 DV(J-1,J)=1.
 1200 CALL MISS (DV,I,9,GAM,1,NER,DET)
      IF (NER .NE. 0) WRITE(6,210)
```

```
C     GAM(1) = TAN(ALPHA), GAM(2) = GAM(1)/COS(ALPHA-- SOLVE FOR GAM(1)
      ALPHA = ATAN(GAM(1))
      CSALF= COS(ALPHA)
      DO 1220 I=1,K
 1220 GAM(I)=GAM(I+1)* CSALF
      GO TO 5000
 2000 CL1=0.0
      DO 2020 I=1,K
 2020 CL1=CL1+ GAM(I)
      CL1= 2.*CL1
      IF ( ABS(CL-CL1) .LT. .0005) GO TO 5000
      ALF1=0.0
      ALF2=.2*(CL-CL1)
      ITER=0
 2050 CSALF = COS(ALF2)
      SNALF=SIN(ALF2)
      M=1
      N= ND(1)-1
      DO 2100 I=1,NB
      GAM(I)=(XTEMP(M)+XTEMP(N))*CSALF
      GAM(I)= -( GAM(I)+(YTEMP(M)+YTEMP(N))*SNALF)
      M=N+1
 2100 N=N+ND(I+1)-1
      DO 2150 I=1,NB
      DO 2150 J=1,NB
 2150 DVA(I,J)=DVX(I,J)
      DET=1.
      CALL MISS (DVA,NB,9,GAM,1,NER,DET)
      IF(NER .NE. 0) WRITE(6,210)
      CL2=0.
      DO 2200 J=1,K
 2200 CL2=CL2+GAM(J)
      CL2=CL2*2.0
      IF(ABS(CL2-CL) .LT. .0005 ) GO TO 2600
      ITER=ITER+1
      IF( ITER .GE. 20) GO TO 2550
      T=ALF1*(CL2-CL)/(CL2-CL1)+ALF2*(CL-CL1)/(CL2-CL1)
      ALF1=ALF2
      ALF2=T
      CL1=CL2
      GO TO 2050
 2550 WRITE(6,500)
 2600 ALPHA=ALF2
 5000 IF(K .EQ. NB) GO TO 5040
      M= NCFLG-1
      DO 5020 I=M,NB
 5020 GAM(I)=0.
 5040 READ(11) (XTEMP(I),I=1,NT)
      SNALF=SIN(ALPHA)
      READ(11) (YTEMP(I),I=1,NT)
      DO 5070 I=1,NT
 5070 VC(I)=XTEMP(I)*CSALF+YTEMP(I)*SNALF
      IF ( K .EQ. 0) GO TO 5150
```

```
      DO 5100 L=1,K
      READ(11) (XTEMP(I),I=1,NT)
      DO 5100 I=1,NT
5100  VC(I)=VC(I)+XTEMP(I)*GAM(L)
5150  M=1
      N=ND(1)-1
      M1=1
      N1=ND(1)
      DO 5250 J=1,NB
      READ(4) (SINA(I),I=M,N)
      READ(4) (COSA(I),I=M,N)
      READ(13)(X(I),I=M1,N1)
      READ(13)(Y(I),I=M1,N1)
      READ(13)(XMP(I),I=M,N)
      READ(13)(YMP(I),I=M,N)
      M1=N1+1
      N1=N1+ND(J+1)
      M=N+1
5250  N=N+ND(J+1)-1
      GT=0.
      DO 5350 I=1,K
5350  GT=GT+GAM(I)
      T=GT/SP*.5
      IF(FLGD5 .EQ. 0 ) FALPHA=ATAN2 (SNALF+T,CSALF)
      ALFEX=ATAN2 (SNALF-T,CSALF)
      ALFEX=ALFEX*57.29578
      FALPHA=FALPHA*57.29578
      ALPHA=ALPHA*57.29578
      IF(FLGD4 .EQ. 0) DALFA=FALPHA-ALFEX
      VIN=SQRT(1.+2.*SNALF*T+T*T)
      VEX=SQRT(1.-2.*SNALF*T+T*T)
      J=1
      K1=1
      M=1
      N=ND(1)-1
      DO 5800 L=1,NB
      K2=ND(L)
      LCTR=19
      ALPI=FALPHA/57.29578
      AEXT=ALFEX/57.29578
      VEXIT=COS(ALPI)/COS(AEXT)
      VTHET=SIN(ALPI)-(VEXIT*SIN(AEXT))
      UIDUA=1.0/SQRT((COS(ALPI)**2)+(((VTHET/2.0)+(VEXIT*SIN(AEXT)))**2)
     *)
      DO 5400 I=M,N
      IP1=I+1
      VC(I)=VC(I)/UIDUA/COS(ALPI)*RS/((R(I)+R(IP1))/2.0)
      CP(I)=1.0-VC(I)**2
5400  CONTINUE
      FX=0.0
      FY=0.0
      CMO=0.0
      DO 5410 I=M,N
```

```
      IP1=I+1
      FY=FY+CP(I)*(X(IP1)-X(I))/100.0
      FX=FX+CP(I)*(Y(I)-Y(IP1))/100.0
      CMO=CMO+CP(I)*((X(IP1)-X(I))*XMP(I)/10000.0-
     1(Y(I)-Y(IP1))*YMP(I)/10000.0)
 5410 CONTINUE
      WGAR=WGA*PI/180.0
      CFTH=(-FX)*SIN(WGAR)-FY*COS(WGAR)
      CFR=FY*SIN(WGAR)-FX*COS(WGAR)
      CMRS=CMO+FX*YS-FY*XS
      I=1
 5501 WRITE(6,601)
  601 FORMAT('1',25X,'APPLIED RESEARCH LABORATORY'/26X,
     1'GARFIELD THOMAS WATER TUNNEL'//)
      WRITE(6,602)HEDR
  602 FORMAT(' ',2X,20A4/)
      WRITE(6,603)NWG,WGA
  603 FORMAT(' ',2X,'NUMBER OF WICKET GATES = ',I2,10X,
     1'WICKET GATE ANGLE = ',F6.2/)
      WRITE(6,604)RS,XS,YS
  604 FORMAT(' ',2X,'RS = ',F10.7,16X,'XS = ',F10.7,12X,'YS = ',F10.7/)
      FALPHN=-FALPHA
      ALFEXN=-ALFEX
      WRITE(6,605)FALPHN,ALFEXN
  605 FORMAT(' ',2X,'INLET FLOW ANGLE = ',F11.7,7X,
     1'EXIT FLOW ANGLE = ',F11.7/)
      WRITE(6,606)CFTH,CFR,CMRS
  606 FORMAT(' ',2X,'CF THETA = ',F11.7, 9X,'CF R = ',F11.7, 9X,
     1'CM = ',F11.7//)
      WRITE(6,607)
  607 FORMAT(' ',T20,'X',T35,'Y',T47,'V/VRS',T62,'CP')
 5600 ABSVC=ABS(VC(K1))
      WRITE(6,608)I,X(J),Y(J),XMP(K1),YMP(K1),ABSVC,CP(K1)
  608 FORMAT(' ',2X,I3,T13,2F14.8/T13,4F14.8)
      I=I+1
      J=J+1
      K1=K1+1
      IF(I.EQ.K2)GO TO 5700
      IF(I.LE.LCTR)GO TO 5600
      LCTR=LCTR+19
      GO TO 5501
 5700 WRITE(6,608)I,X(J),Y(J)
      J=J+1
      M=N+1
 5800 N=N+ND(L+1)-1
C     K= NCFLG-2 =NUMBER OF GAMMAS
      IF(FLGO2 .EQ. 0) GO TO 9191
      N=ND(NB+1)
      READ(3) (XTEMP(I), I=1,NT )
      READ(3) (YTEMP(I), I=1,NT )
      DO 5870 I=1,NT
 5870 SIGT(I)=XTEMP(I)*CSALF+YTEMP(I)*SNALF
      IF (K .EQ. 0 ) GO TO 6150
```

```
      DO 6000 J=1,K
      READ(4)
      READ(4)
C ** PRECEDING 2 READS WILL SKIP ON-BODY NON-UNIFORM ONSET FLOW
      READ(3) (XTEMP(I),I=1,NT)
      DO 6000 I=1,NT
 6000 SIGT(I)=SIGT(I) + XTEMP(I)*GAM(J)
      M=1
      M1=N
      DO 6100 J=1,K
      READ(4) (XTEMP(I),I=M,M1)
      READ(4) (YTEMP(I),I=M,M1)
      M=M1+1
 6100 M1=M1+N
 6150 DO 6400 J=1,N
      READ(10) (YIJ(I),I=1,NT)
      READ(10) (XIJ(I),I=1,NT)
      SUM1=0.0
      SUM2=0.0
      DO 6200 I=1,NT
      T=SIGT(I)
      SUM1=SUM1+T*XIJ(I)
 6200 SUM2=SUM2+T*YIJ(I)
      IF(K .EQ. 0) GO TO 6300
      N1=J
      DO 6250 I=1,K
      T=GAM(I)
      SUM1=SUM1+T*YTEMP(N1)
      SUM2=SUM2+T*XTEMP(N1)
 6250 N1=N1+N
 6300 VXL(J)=SUM1+CSALF
 6400 VYL(J)=SUM2+SNALF
      LCTR=45
      IOB=1
      DO 6450 L=1,NB
      IOB=IOB+ND(L)
 6450 CONTINUE
      DO 6460 J=1,N
      IIOB=IOB+J-1
      VXL(J)=(-VXL(J))*RS/R(IIOB)/UIOUA/COS(ALPI)
      VYL(J)=VYL(J)*RS/R(IIOB)/UIOUA/COS(ALPI)
 6460 CONTINUE
C     VXL NOW REPRESENTS VR
C     VYL NOW REPRESENTS V THETA
      IOB2=IOB+N-1
      READ(13)(X(I),I=IOB,IOB2)
      READ(13)(Y(I),I=IOB,IOB2)
C     X REPRESENTS R
C     Y REPRESENTS THETA
      I=1
 6500 WRITE(6,601)
      WRITE(6,602)HEDR
      WRITE(6,610)
```

```
 610 FORMAT('0',2X,'OFF-BODY POINT VELOCITIES'/)
     WRITE(6,611)
 611 FORMAT(' ',T20,'R',T33,'THETA',T47,'VR/VRS',T58,'VTHETA/VRS'/)
6600 WRITE(6,612)I,X(IOB),Y(IOB),VXL(I),VYL(I)
 612 FORMAT(' ',2X,I3,T13,4F14.8)
     IOB=IOB+1
     I=I+1
     IF(I .GT. N) GO TO 9191
     IF( I .LE. LCTR) GO TO 6600
     LCTR=LCTR+45
     GO TO 6500
9191 RETURN
     END
```

```
      SUBROUTINE FORM1 (J,K,J2,Z,Q,SINA,COSA,W)
      COMMON IM,NER,NT,NB,NCFLG,RPI,R2PI,SP,CL,ALPHA,FALPHA
     1,DALFA,CHORD,FLG02,FLG03,FLG04,FLG05,FLG06,FLG07,FLG08,FLG09,
     2FLG10,FLG11,FLG12,ND,NLF,SUMDS,XS,YS,RS,WGA,NWG
      DIMENSION ND(10),NLF(10),SUMDS(10),XMC(8),YMC(8),ADDY(8)
      COMPLEX IM,Z,Q,W,CLOG
      DIMENSION Z(100),Q(100),SINA(100),COSA(100)
      W=CLOG((Z(J)-Q(K))/(Z(J)-Q(K+1)))
      W=(COSA(J2)-IM*SINA(J2))*R2PI*W
      RETURN
      END
      SUBROUTINE FORM2 (J,K,J2,Z,Q,SINA,COSA,W)
      COMMON IM,NER,NT,NB,NCFLG,RPI,R2PI,SP,CL,ALPHA,FALPHA
     1,DALFA,CHORD,FLG02,FLG03,FLG04,FLG05,FLG06,FLG07,FLG08,FLG09,
     2FLG10,FLG11,FLG12,ND,NLF,SUMDS,XS,YS,RS,WGA,NWG
      DIMENSION ND(10),NLF(10),SUMDS(10),XMC(8),YMC(8),ADDY(8)
      COMPLEX IM,Z,Q,W,CLOG
      DIMENSION Z(100),Q(100),SINA(100),COSA(100)
      W=CLOG(Z(J)-CONJG(Q(K)))/(Z(J)-CONJG(Q(K+1)))
      W=(COSA(J2)+IM*SINA(J2))*R2PI*W
      RETURN
      END
      SUBROUTINE SPGTO (J,K,J2,SP,TF,Z,Q,SINA,COSA,W)
      COMMON IM,NER,NT,NB,NCFLG,RPI,R2PI
      COMPLEX IM,Z,Q,W,TF,TN,CLOG,CSINH
      DIMENSION Z(100),Q(100),SINA(100),COSA(100)
      TN=CSINH(3.14159*(Z(J)-Q(K+1))/SP)
      W=(COSA(J2) -IM*SINA(J2))*CLOG(TF/TN)*R2PI
      TF=TN
      RETURN
      END
      COMPLEX FUNCTION CSINH(Z)
      COMPLEX Z
      CSINH=(CEXP(Z)-CEXP(-Z))/2.0
      RETURN
      END
      SUBROUTINE MIS1 (A,N, NDD,B,M,NERR,D)
      DIMENSION A(18225),B(1350)
      NERR=1
      ND=NDD
   10 DO 90 I=1,N
      AIJMAX=A(I)
      IJMAX=I
      DO 25 J=2,N
      IJ=I+(J-1)*ND
      IF (ABS(A(IJ))-ABS(AIJMAX)) 25,25,20
   20 AIJMAX=A(IJ)
      IJMAX=IJ
   25 CONTINUE
      IF (AIJMAX) 30,999,30
   30 DO 35 J=1,N
      IJ=I+(J-1)*ND
   35 A(IJ)=A(IJ)/AIJMAX
```

```
      D=D*AIJMAX
      DO 40 J=1,M
      IJ=I+(J-1)*ND
   40 B(IJ)=B(IJ)/AIJMAX
      DO 70 K=1,N
      IF (K-I) 50,70,50
   50 KJMAX=IJMAX+(K-I)
      ARAT=-A(KJMAX)
      KJ=K
      IJ=I
      DO 60 J=1,N
      IF (A(IJ)) 55,58,55
   55 A(KJ)=ARAT*A(IJ)+A(KJ)
   58 KJ=KJ+ND
   60 IJ=IJ+ND
      A(KJMAX)=0.0
      KJ=K
      IJ=I
      DO 69 J=1,M
      IF (B(IJ)) 65,68,65
   65 B(KJ)=ARAT*B(IJ)+B(KJ)
   68 KJ=KJ+ND
69    IJ=IJ+ND
   70 CONTINUE
      KJ=IJMAX-I+1
      FI = I
   90 A(KJ)=FI
      DO 100 I=1,N
      K=I
   93 I1=K*ND-ND+1
      FK=A(I1)
      K = FK
      IF(K-I) 93,100,95
   95 IJ=I
      IK=K
      DO 99 J=1,M
      A(2)=B(IJ)
      B(IJ)=B(IK)
      B(IK)=A(2)
      IJ=IJ+ND
   99 IK=IK+ND
  100 CONTINUE
      NERR=0
  999 RETURN
      END
      SUBROUTINE MISS (A,N, NDD, B, M, NERR,D)
      DIMENSION A(81),B(9)
      NERR=1
      ND=NDD
   10 DO 90 I=1,N
      AIJMAX = A(I)
      IJMAX= I
      DO 25 J=2,N
```

```
      IJ=I+(J-1)*ND
      IF ( ABS(A(IJ))- ABS(AIJMAX)) 25,25,20
   20 AIJMAX=A(IJ)
      IJMAX=IJ
   25 CONTINUE
      IF (AIJMAX) 30,999,30
   30 DO 35 J=1,N
      IJ=I + (J-1)*ND
   35 A(IJ)=A(IJ)/AIJMAX
       D=D*AIJMAX
      DO 40 J=1,M
      IJ=I+(J-1)*ND
   40 B(IJ)=B(IJ)/AIJMAX
      DO 70 K=1,N
      IF(K-I) 50,70,50
   50 KJMAX = IJMAX + (K-I)
      ARAT= -A(KJMAX)
      KJ=K
      IJ=I
      DO 60 J=1,N
      IF(A(IJ)) 55,58,55
   55 A(KJ) = ARAT*A(IJ) +A(KJ)
   58 KJ=KJ+ND
   60 IJ=IJ+ND
      A(KJMAX)=0.0
      KJ=K
      IJ=I
      DO 69 J=1,M
      IF (B(IJ)) 65,68,65
   65 B(KJ)=ARAT*B(IJ)+B(KJ)
   68 KJ=KJ+ND
   69 IJ=IJ+ND
   70 CONTINUE
      KJ=IJMAX-I+1
      FI = I
   90 A(KJ) = FI
      DO 100 I=1,N
      K=I
   93 II= K*ND-ND+1
      FK = A(II)
      K = FK
      IF (K-I) 93,100,95
   95 IJ=I
      IK=K
      DO 99 J=1,M
      A(2)=B(IJ)
      B(IJ)=B(IK)
      B(IK)=A(2)
      IJ=IJ+ND
   99 IK=IK+ND
  100 CONTINUE
      NERR=0
  999 RETURN
      END
```

INPUT LISTING

```
//DATA.INPUT DD *
SAMPLE PROBLEM FOR CAMBERED WICKET GATE
1000
   89    10  0.0
   45    20  60.0     60.0       3.0201232 .5461218  .031533282
 100.00000   0.00000
  99.89999   0.72468
  99.75000   1.12923
  99.50000   1.55734
  99.00000   2.08582
  98.50000   2.40332
  98.00000   2.58885
  97.50000   2.72502
  96.75000   2.92638
  95.50000   3.25439
  94.00000   3.63549
  92.50000   4.00300
  88.50000   4.91747
  81.50000   6.29158
  73.50000   7.51657
  65.50000   8.38015
  57.50000   8.88750
  49.50000   9.04165
  45.50000   8.98663
  41.50000   8.84343
  37.50000   8.61195
  33.50000   8.29176
  29.50000   7.88243
  25.50000   7.38332
  21.50000   6.79372
  17.50000   6.11269
  13.50000   5.33925
  10.50000   4.69776
   8.50000   4.24055
   7.00000   3.88200
   6.00000   3.63549
   5.00000   3.38292
   4.00000   3.12432
   3.00000   2.85966
   2.25000   2.65711
   1.75000   2.51020
   1.50000   2.40332
   1.25000   2.26402
   1.00000   2.08582
   0.75000   1.85754
   0.50000   1.55734
   0.25000   1.12923
   0.15000   0.88323
   0.05000   0.51481
   0.00000   0.00000
   0.05000  -0.51481
   0.15000  -0.88323
   0.25000  -1.12923
   0.50000  -1.55734
   0.75000  -1.85754
   1.00000  -2.08582
   1.25000  -2.26402
   1.50000  -2.40332
   1.75000  -2.51020
   2.25000  -2.64129
   3.00000  -2.67532
   4.00000  -2.67532
   5.00000  -2.67532
   6.00000  -2.67532
   7.00000  -2.67532
   8.50000  -2.67532
```

```
 10.50000  -2.67532
 13.50000  -2.67532
 17.50000  -2.67532
 21.50000  -2.67532
 25.50000  -2.67532
 29.50000  -2.67532
 33.50000  -2.67532
 37.50000  -2.67532
 41.50000  -2.67532
 45.50000  -2.67532
 49.50000  -2.67532
 57.50000  -2.67532
 65.50000  -2.67532
 73.50000  -2.67532
 81.50000  -2.67532
 88.50000  -2.67532
 92.50000  -2.67532
 94.00000  -2.67532
 95.50000  -2.67532
 96.75000  -2.67532
 97.50000  -2.66957
 98.00000  -2.58868
 98.50000  -2.40332
 99.00000  -2.08582
 99.50000  -1.55734
 99.75000  -1.12923
 99.89999  -0.72468
100.00000   0.00000
```

```
    10    00  0.0
  5.0         0.0
  5.0         4.5
  5.0         9.0
  5.0         13.5
  5.0         18.0
  1.0         0.0
  1.0         4.5
  1.0         9.0
  1.0         13.5
  1.0         18.0

    1
```

SAMPLE OUTPUT

INPUT PARAMETERS

```
FLGO2 = 1
FLGO8 = 0
FLGO9 = 0
FLG12 = 0
NN =  89
BDN = 1
SUBKS = 0
ROPFB =  0.0000000
NLE = 45
NWG = 20
WGA =  60.00000
FALPHA =  60.00000
RS =  3.0201230
XS =  0.5461218
YS =  0.0315333
NN =  10
BDN = 0
SUBKS = 0
ROPFB =  0.0000000
```

APPLIED RESEARCH LABORATORY
GARFIELD THOMAS WATER TUNNEL

SAMPLE PROBLEM FOR CAMBERED WICKET GATE

NUMBER OF WICKET GATES = 20 WICKET GATE ANGLE = 60.00

RS = 3.0201230 XS = 0.5461218 YS = 0.0315333

INLET FLOW ANGLE = 59.9999600 EXIT FLOW ANGLE = 64.9216400

CF THETA = 0.7893797 CF R = -1.8414580 CM = 0.0215683

	X	Y	V/VRS	CP
1	100.00000000	0.00000000		
	99.94999000	0.36233990	0.59471640	0.64631240
2	99.89999000	0.72468000		
	99.82499000	0.92695470	1.48706200	-1.21135400
3	99.75000000	1.12922900		
	99.62500000	1.34328400	2.03884300	-3.15688100
4	99.50000000	1.55733900		
	99.25000000	1.82157900	2.60373400	-5.77943500
5	99.00000000	2.08582000		
	98.75000000	2.24456900	3.03379800	-8.20393000
6	98.50000000	2.40332000		
	98.25000000	2.49608500	3.03894900	-8.23521000
7	98.00000000	2.58885000		
	97.75000000	2.65693400	2.82446100	-6.97758400
8	97.50000000	2.72502000		
	97.12500000	2.82569900	2.65828200	-6.06646400
9	96.75000000	2.92638000		
	96.12500000	3.09038400	2.56366100	-5.58775200
10	95.50000000	3.25438900		
	94.75000000	3.44493900	2.50539700	-5.27701700
11	94.00000000	3.63549000		
	93.25000000	3.81924500	2.47368700	-5.11912700
12	92.50000000	4.00300000		
	90.50000000	4.46023400	2.44061500	-4.95660400
13	88.50000000	4.91746900		
	85.00000000	5.60452400	2.39334600	-4.72810800
14	81.50000000	6.29158000		
	77.50000000	6.90407400	2.34706900	-4.50873500
15	73.50000000	7.51657000		
	69.50000000	7.94835900	2.29603700	-4.27178800
16	65.50000000	8.38014900		
	61.50000000	8.63381900	2.24320400	-4.03196400
17	57.50000000	8.88749900		
	53.50000000	8.96456900	2.19073600	-3.79932600
18	49.50000000	9.04164900		
	47.50000000	9.01413700	2.16501600	-3.68729400
19	45.50000000	8.98663000		
	43.50000000	8.91502300	2.13801400	-3.57110600

APPLIED RESEARCH LABOFATORY
GARFIELD THOMAS WATER TUNNEL

SAMPLE PROBLEM FOR CAMBERED WICKET GATE

NUMBER OF WICKET GATES = 20 WICKET GATE ANGLE = 60.00

RS = 3.0201230 XS = 0.5461218 YS = 0.0315333

INLET FLOW ANGLE = 59.9999600 EXIT FLOW ANGLE = 64.9216400

CF THETA = 0.7893797 CF R = -1.8414580 CM = 0.0215683

	X	Y	V/VRS	CP
20	41.50000000	8.84342000		
	39.50000000	8.72768400	2.11223900	-3.46155600
21	37.50000000	8.61194000		
	35.50000000	8.45185000	2.08615400	-3.35204200
22	33.50000000	8.29176000		
	31.50000000	8.08708900	2.05917000	-3.24018300
23	29.50000000	7.88243000		
	27.50000000	7.63287400	2.03085500	-3.12437200
24	25.50000000	7.38331900		
	23.50000000	7.08852000	2.00085800	-3.00343300
25	21.50000000	6.79372000		
	19.50000000	6.45320500	1.96874400	-2.87595300
26	17.50000000	6.11268900		
	15.50000000	5.72596900	1.93411000	-2.74078300
27	13.50000000	5.33924900		
	12.00000000	5.01850400	1.90652100	-2.63482400
28	10.50000000	4.69775900		
	9.50000000	4.46915400	1.88791200	-2.56421300
29	8.50000000	4.24055000		
	7.75000000	4.06127400	1.87614100	-2.51990600
30	7.00000000	3.88199900		
	6.50000000	3.75874500	1.86979700	-2.49614300
31	6.00000000	3.63549000		
	5.50000000	3.50920400	1.86927700	-2.49419900
32	5.00000000	3.38292000		
	4.50000000	3.25362000	1.87734700	-2.52443500
33	4.00000000	3.12432000		
	3.50000000	2.99199000	1.90670700	-2.63553400
34	3.00000000	2.85966000		
	2.62500000	2.75838400	1.97394200	-2.89644900
35	2.25000000	2.65711000		
	2.00000000	2.58365400	2.11068000	-3.45497200
36	1.75000000	2.51019900		
	1.62500000	2.45675900	2.23801600	-4.00871500
37	1.50000000	2.40332000		
	1.37500000	2.33366900	2.22070800	-3.93154700
38	1.25000000	2.26401900		
	1.12500000	2.17492000	2.13881400	-3.57452800

APPLIED RESEARCH LABORATORY
GARFIELD THOMAS WATER TUNNEL

SAMPLE PROBLEM FOR CAMBERED WICKET GATE

NUMBER OF WICKET GATES = 20 WICKET GATE ANGLE = 60.00

RS = 3.0201230 XS = 0.5461218 YS = 0.0315333

INLET FLOW ANGLE = 59.9999600 EXIT FLOW ANGLE = 64.9216400

CF THETA = 0.7893797 CF R = -1.8414580 CM = 0.0215683

	X	Y	V/VRS	CP
39	1.00000000	2.08582000		
	0.87500000	1.97167900	1.98831800	-2.95341000
40	0.75000000	1.85754000		
	0.62500000	1.70743900	1.75195100	-2.06933200
41	0.50000000	1.55733900		
	0.37500000	1.34328400	1.36447700	-0.86179730
42	0.25000000	1.12922900		
	0.19999990	1.00622900	1.02807900	-0.05694771
43	0.14999990	0.88322990		
	0.09999996	0.69901990	0.69075520	0.52285710
44	0.05000000	0.51481000		
	0.02500000	0.25740490	0.16441660	0.97296720
45	0.00000000	0.00000000		
	0.02500000	-0.25740490	0.46612930	0.78272340
46	0.05000000	-0.51481000		
	0.09999996	-0.69901990	1.01965300	-0.03969288
47	0.14999990	-0.88322990		
	0.19999990	-1.00622900	1.39530800	-0.94688510
48	0.25000000	-1.12922900		
	0.37500000	-1.34328400	1.78914300	-2.20103400
49	0.50000000	-1.55733900		
	0.62500000	-1.70743900	2.26682300	-4.13848900
50	0.75000000	-1.85754000		
	0.87500000	-1.97167900	2.58995300	-5.70785800
51	1.00000000	-2.08582000		
	1.12500000	-2.17492000	2.82889200	-7.00263300
52	1.25000000	-2.26401900		
	1.37500000	-2.33366900	3.00371900	-8.02232900
53	1.50000000	-2.40332000		
	1.62500000	-2.45675900	3.13212800	-8.81023000
54	1.75000000	-2.51019900		
	2.00000000	-2.57574400	3.12789900	-8.78375200
55	2.25000000	-2.64128900		
	2.62500000	-2.65830400	2.88813000	-7.34129500
56	3.00000000	-2.67531900		
	3.50000000	-2.67531900	2.60166300	-5.76865200
57	4.00000000	-2.67531900		
	4.50000000	-2.67531900	2.45468200	-5.02546500

APPLIED RESEARCH LABORATORY
GARFIELD THOMAS WATER TUNNEL

SAMPLE PROBLEM FOR CAMBERED WICKET GATE

NUMBER OF WICKET GATES = 20 WICKET GATE ANGLE = 60.00

RS = 3.0201230 XS = 0.5461218 YS = 0.0315333

INLET FLOW ANGLE = 59.9999600 EXIT FLOW ANGLE = 64.9216400

CF THETA = 0.7893797 CF R = -1.8414580 CM = 0.0215683

	X	Y	V/VRS	CP
58	5.00000000	-2.67531900		
	5.50000000	-2.67531900	2.38719300	-4.69869300
59	6.00000000	-2.67531900		
	6.50000000	-2.67531900	2.34865800	-4.51619600
60	7.00000000	-2.67531900		
	7.75000000	-2.67531900	2.32482800	-4.40482500
61	8.50000000	-2.67531900		
	9.50000000	-2.67531900	2.30727800	-4.32353400
62	10.50000000	-2.67531900		
	12.00000000	-2.67531900	2.30145900	-4.29671400
63	13.50000000	-2.67531900		
	15.50000000	-2.67531900	2.30795200	-4.32664500
64	17.50000000	-2.67531900		
	19.50000000	-2.67531900	2.32270200	-4.39494600
65	21.50000000	-2.67531900		
	23.50000000	-2.67531900	2.34291100	-4.48923400
66	25.50000000	-2.67531900		
	27.50000000	-2.67531900	2.36626000	-4.59918800
67	29.50000000	-2.67531900		
	31.50000000	-2.67531900	2.39180700	-4.72074300
68	33.50000000	-2.67531900		
	35.50000000	-2.67531900	2.41912300	-4.85215800
69	37.50000000	-2.67531900		
	39.50000000	-2.67531900	2.44811500	-4.99326800
70	41.50000000	-2.67531900		
	43.50000000	-2.67531900	2.47842900	-5.14261300
71	45.50000000	-2.67531900		
	47.50000000	-2.67531900	2.50940600	-5.29711800
72	49.50000000	-2.67531900		
	53.50000000	-2.67531900	2.55813000	-5.54403000
73	57.50000000	-2.67531900		
	61.50000000	-2.67531900	2.62046300	-5.86682700
74	65.50000000	-2.67531900		
	69.50000000	-2.67531900	2.68101300	-6.18783000
75	73.50000000	-2.67531900		
	77.50000000	-2.67531900	2.74073200	-6.51161200
76	81.50000000	-2.67531900		
	85.00000000	-2.67531900	2.80448900	-6.86515900

APPLIED RESEARCH LABORATORY
GARFIELD THOMAS WATER TUNNEL

SAMPLE PROBLEM FOR CAMBERED WICKET GATE

NUMBER OF WICKET GATES = 20 WICKET GATE ANGLE = 60.00

RS = 3.0201230 XS = 0.5461218 YS = 0.0315333

INLET FLOW ANGLE = 59.9999600 EXIT FLOW ANGLE = 64.9216400

CF THETA = 0.7893797 CF R = -1.8414580 CM = 0.0215683

	X	Y	V/VRS	CP
77	88.50000000	-2.67531900		
	90.50000000	-2.67531900	2.87847300	-7.28560800
78	92.50000000	-2.67531900		
	93.25000000	-2.67531900	2.94663900	-7.68268100
79	94.00000000	-2.67531900		
	94.75000000	-2.67531900	3.04412200	-8.26668200
80	95.50000000	-2.67531900		
	96.12500000	-2.67531900	3.22393400	-9.39375100
81	96.75000000	-2.67531900		
	97.12500000	-2.67244400	3.56036800	-11.67622000
82	97.50000000	-2.66956900		
	97.75000000	-2.62912400	3.95477400	-14.64024000
83	98.00000000	-2.58868000		
	98.25000000	-2.49600000	3.96366200	-14.71061000
84	98.50000000	-2.40332000		
	98.75000000	-2.24456900	3.65976400	-12.39387000
85	99.00000000	-2.08582000		
	99.25000000	-1.82157900	2.96567700	-7.79524100
86	99.50000000	-1.55733900		
	99.62500000	-1.34328400	2.20933500	-3.88116100
87	99.75000000	-1.12922900		
	99.82499000	-0.92695470	1.55355800	-1.41354200
88	99.89999000	-0.72468000		
	99.94999000	-0.36233990	0.59613400	0.64462420
89	100.00000000	0.00000000		

APPLIED RESEARCH LABORATORY
GARFIELD THOMAS WATER TUNNEL

SAMPLE PROBLEM FOR CAMBERED WICKET GATE

OFF-BODY POINT VELOCITIES

	R	THETA	VR/VRS	VTHETA/VRS
1	5.00000000	0.00000000	-0.60478180	-1.04622200
2	5.00000000	4.50000000	-0.60474200	-1.04621200
3	5.00000000	9.00000000	-0.60475190	-1.04617300
4	5.00000000	13.50000000	-0.60479180	-1.04618200
5	5.00000000	18.00000000	-0.60478220	-1.04622200
6	1.00000000	0.00000000	-3.01638100	-6.45360400
7	1.00000000	4.50000000	-3.01638100	-6.45360600
8	1.00000000	9.00000000	-3.01638300	-6.45360400
9	1.00000000	13.50000000	-3.01637900	-6.45360400
10	1.00000000	18.00000000	-3.01638100	-6.45360400

INPUT PARAMETERS

FLG02 = 0
FLG08 = 0
FLG09 = 0
FLG12 = 1

END OF PROGRAM - DATA HAS BEEN EXHAUSTED

GPO 859-331